

ดีไฮเดรชันของ 1,2-โพรเพนไดออกไซด์เป็นโพรพานอลและโพรพานอนโดยใช้ตัวเร่งปฏิกิริยา
H-ZSM-5 และ H-MOR ด้วยวิธี ONIOM

นางสาวอรุณวรรณ จันทร์เสน

วิทยานิพนธ์นี้เป็นส่วนหนึ่งของการศึกษาตามหลักสูตรปริญญาวิทยาศาสตรมหาบัณฑิต
สาขาวิชาปิโตรเคมีและวิทยาศาสตร์พอลิเมอร์
คณะวิทยาศาสตร์ จุฬาลงกรณ์มหาวิทยาลัย
ปีการศึกษา 2555
ลิขสิทธิ์ของจุฬาลงกรณ์มหาวิทยาลัย

บทคัดย่อและแฟ้มข้อมูลฉบับเต็มของวิทยานิพนธ์ตั้งแต่ปีการศึกษา 2554 ที่ให้บริการในคลังปัญญาจุฬาฯ (CUIR)
เป็นแฟ้มข้อมูลของนิสิตเจ้าของวิทยานิพนธ์ที่ส่งผ่านทางบัณฑิตวิทยาลัย

The abstract and full text of theses from the academic year 2011 in Chulalongkorn University Intellectual Repository (CUIR)
are the thesis authors' files submitted through the Graduate School.

DEHYDRATION OF 1,2-PROPANEDIOL TO PROPANAL AND PROPANONE
USING H-ZSM-5 AND H-MOR CATALYSTS BY ONIOM METHOD

Miss Arunwan Jansen

A Thesis Submitted in Partial Fulfillment of the Requirements
for the Degree of Master of Science Program in Petrochemistry and Polymer Science
Faculty of Science
Chulalongkorn University
Academic Year 2012
Copyright of Chulalongkorn University

Thesis Title DEHYDRATION OF 1,2-PROPANEDIOL TO PROPANAL
AND PROPANONE USING H-ZSM-5 AND H-MOR
CATALYSTS BY ONIOM METHOD

By Miss Arunwan Jansen

Field of study Petrochemistry and Polymer Science

Thesis Advisor Associate Professor Vithaya Ruangpornvisuti, Dr.rer.nat.

Accepted by the Faculty of Science, Chulalongkorn University in Partial
Fulfillment of the Requirements for the Master's Degree

.....Dean of the Faculty of Science
(Professor Supot Hannongbua, Dr.rer.nat.)

THESIS COMMITTEE

.....Chairman
(Assistant Professor Warinthorn Chavasiri, Ph.D.)

.....Thesis Advisor
(Associate Professor Vithaya Ruangpornvisuti, Dr.rer.nat.)

.....Examiner
(Assistant Professor Somsak Pianwanit, Ph.D.)

.....External Examiner
(Assistant Professor Khajadpai Thipyapong, Ph.D.)

อรุณวรรณ จันทร์เสน : ดีไฮเดรชันของ 1,2-โพรเพนไดออลเป็นโพรพานาลและโพรพาโนนโดยใช้ตัวเร่งปฏิกิริยา H-ZSM-5 และ H-MOR ด้วยวิธี ONIOM. (DEHYDRATION OF 1,2-PROPANEDIOL TO PROPANAL AND PROPANONE USING H-ZSM-5 AND H-MOR CATALYSTS BY ONIOM METHOD) อ. ที่ปรึกษาวิทยานิพนธ์หลัก: รศ.ดร.วิทยา เรืองพรวิสุทธิ, 55 หน้า.

ปฏิกิริยาที่เกิดขึ้นบนตัวเร่งปฏิกิริยา H-ZSM-5, H-MOR และ H-TON มีลักษณะเฉพาะของตัวเร่งปฏิกิริยาแต่ละตัว โดยปฏิกิริยาการเปลี่ยน 1,2-โพรเพนไดออลเป็นโพรพานาล ประกอบด้วยสามขั้นตอน และการเปลี่ยนเป็นโพรพาโนนประกอบด้วยสี่ขั้นตอน กลไกการเกิดปฏิกิริยาดีไฮเดรชันของ 1,2-โพรเพนไดออลเป็นโพรพานาลและโพรพาโนนบนคลัสเตอร์ของตัวเร่งปฏิกิริยา H-ZSM-5, H-MOR และ H-TON ศึกษาด้วยวิธี ONIOM (B3LYP/6-31+G(d):AM1) และหาสมบัติทางเทอร์โมไดนามิกส์ ค่าพลังงาน ค่าคงที่อัตราเร็ว และค่าคงที่ของสมดุลของการเปลี่ยน 1,2-โพรเพนไดออลเป็นโพรพานาล และโพรพาโนนบนตัวเร่งปฏิกิริยา H-ZSM-5, H-MOR และ H-TON ที่อุณหภูมิ 298.15 เคลวิน พบว่าค่าคงที่อัตราเร็วของการเปลี่ยน 1,2-โพรเพนไดออลเป็นโพรพานาล และการเปลี่ยน 1,2-โพรเพนไดออลเป็นโพรพาโนนบนตัวเร่งปฏิกิริยา H-ZSM-5, H-MOR และ H-TON มีอันดับการลดลงเป็น H-TON > H-ZSM-5 > H-MOR และ H-ZSM-5 > H-MOR > H-TON ตามลำดับ

สาขาวิชา ปิโตรเคมีและวิทยาศาสตร์พอลิเมอร์ ลายมือชื่อนิสิต.....

ปีการศึกษา.....2555.....ลายมือชื่อ อ.ที่ปรึกษาวิทยานิพนธ์หลัก.....

5372385123: PETROCHEMISTRY AND POLYMER SCIENCE PROGRAM
 KEYWORDS: H-ZSM-5, H-MOR AND H-TON ZEOLITES/ 1,2-
 PROPANEDIOL/ PROPANAL AND PROPANONE/ ONIOM

ARUNWAN JANSEN: DEHYDRATION OF 1,2-PROPANEDIOL TO
 PROPANAL AND PROPANONE USING H-ZSM-5 AND H-MOR
 CATALYSTS BY ONIOM METHOD. ADVISOR: ASSOC. PROF.
 VITHAYA RUANGPORNVISUTI, Dr.rer.nat. , 55 pp.

The reaction on H-ZSM-5, H-MOR and H-TON catalysts are individually composed of three steps for 1,2-propanediol conversion to propanal and four steps for conversion to propanone. The reaction mechanisms for dehydration of 1,2-propanediol to propanal and propanone over H-ZSM-5, H-MOR and H-TON catalysts were studied using ONIOM (B3LYP/6-31+G(d):AM1) method. Thermodynamic properties, reaction energies, rate and equilibrium constants of 1,2-propanediol to propanal and propanone over H-ZSM-5, H-MOR and H-TON catalysts reactions were determined at 298.15 K. The rate constants for 1,2-propanediol conversion to propanal and 1,2-propanediol conversion to propanone over H-ZSM-5, H-MOR and H-TON catalysts are in decreasing orders: H-TON > H-ZSM-5 > H-MOR, and H-ZSM-5 > H-MOR > H-TON, respectively.

Field of Study: Petrochemistry and Polymer Science Student's Signature.....

Academic Year: 2012.....Advisor's Signature.....

ACKNOWLEDGEMENTS

This study was performed at the Petrochemistry and Polymer Science, Faculty of Science, Chulalongkorn University. The 90th Anniversary of Chulalongkorn University Fund (Ratchadaphiseksomphot Endowment Fund) provided through the Graduate School, Chulalongkorn University for granted to appreciatively acknowledge to me. I particularly thank advisor Associate Professor Dr. Vithaya Ruangpornvisuti for his advice and invaluable guidance in this thesis.

I would like to thank the committee Assistant Professor Dr. Warinthorn Chavasiri, Assistant Professor Dr. Somsak Pianwanit and Assistant Professor Dr. Khajadpai Thipyapong for their valuable suggestions and comments as committee and thesis examiners.

Special thanks to all members in Supramolecular Chemistry Research Unit for their nice help. I also would like to thank all teaching staff and my friends for all their continuous inspiration, friendship, and good suggestions.

Finally, I would like to thank my family; my mother and father, my aunt, my brother and my sisters for their countless love, always backup and believing in my decisions. I am very full proud to be a part of this family.

CONTENTS

| | Page |
|---|-------------|
| ABSTRACT IN THAI | iv |
| ABSTRACT IN ENGLISH | v |
| ACKNOWLEDGEMENTS | vi |
| CONTENTS | vii |
| LIST OF TABLES | x |
| LIST OF FIGURES | xi |
| LIST OF ABBREVIATIONS AND SYMBOLS | xiv |
| | |
| CHAPTER I INTRODUCTION | 1 |
| | |
| 1.1 Background..... | 1 |
| 1.2 Zeolites..... | 1 |
| 1.2 1 Acidity of zeolites..... | 2 |
| 1.2 2 ZSM-5 zeolite..... | 3 |
| 1.2 3 MOR zeolite..... | 4 |
| 1.2 4 TON zeolite..... | 5 |
| 1.3 Dehydration of 1,2-propanediol..... | 6 |
| 1.4 Objective..... | 7 |
| | |
| CHAPTER II THEORIES | 8 |
| | |
| 2.1 Quantum mechanics in computational chemistry..... | 8 |
| 2.2 Semi-empirical method..... | 8 |
| 2.3 Ab Initio method..... | 9 |
| 2.4 Density functional theory (DFT) methods..... | 9 |
| 2.4.1 Kohn-Sham energy..... | 9 |
| 2.4.2 Kohn-Sham equations | 10 |
| 2.4.3 DFT exchange and correlations..... | 10 |

| | Page |
|---|---------------|
| 2.4.4 Hybrid functions | 11 |
| 2.5 Basis sets..... | 12 |
| 2.5.1 Slater-type orbital (STO)..... | 12 |
| 2.5.2 Gaussian type orbitals (GTO)..... | 13 |
| 2.5.3 Minimal basis sets..... | 13 |
| 2.5.4 Split the valence basis sets | 13 |
| 2.5.5 Polarization basis sets | 13 |
| 2.5.6 Diffuse functions..... | 14 |
| 2.6 The ONIOM method | 14 |
| 2.7 Transition state theory and rate constant | 14 |
| 2.7.1 Rate constant and Boltzman distribution | 15 |
| 2.7.2 Rate constant with tunneling corrections..... | 16 |
| 2.7.3 Partition functions..... | 16 |
| 2.7.3.1 Translation partition function..... | 17 |
| 2.7.3.2 Rotational partition function..... | 17 |
| 2.7.3.3 Vibrational partition function..... | 18 |
| 2.7.3.4 Electronic partition function..... | 18 |
| 2.8 Molecular vibrational frequencies..... | 18 |
| 2.9 Thermochemistry..... | 20 |
| CHAPTER III COMPUTATIONAL DETAILS..... | 22 |
| 3.1. Cluster models for the H-ZSM-5, H-MOR and H-TON | 22 |
| 3.2. Structure optimization and potential energy surface | 23 |
| 3.3 Thermodynamic properties and formation constants | 24 |
| CHAPTER IV RESULTS AND DISCUSSION | 25 |
| 4.1 Optimized structures of zeolite catalysts and involved compounds..... | 25 |
| 4.2 Conversion of 1,2-propanediol over the H-ZSM-5..... | 27 |

| | Page |
|--|-------------|
| 4.3 Conversion of 1,2-propanediol over the H-MOR | 34 |
| 4.4 Conversion of 1,2-propanediol over the H-TON | 41 |
| CHAPTER V CONCLUSIONS | 48 |
| Conclusions..... | 48 |
| REFERENCES | 50 |
| VITAE | 55 |

LIST OF TABLES

| Table | | Page |
|--------------|---|-------------|
| 4.1 | Reaction energies, thermodynamic properties, rate constants and equilibrium constants for conversion reactions of 1,2-propanediol (PG) to propanone (PNE) and propanal (PNL) over the H-ZSM-5 catalyst..... | 33 |
| 4.2 | Reaction energies, thermodynamic properties, rate constants and equilibrium constants for conversion reactions of 1,2-propanediol (PG) to propanone (PNE) and propanal (PNL) over the H-MOR catalyst..... | 40 |
| 4.3 | Reaction energies, thermodynamic properties, rate constants and equilibrium constants for conversion reactions of 1,2-propanediol (PG) to propanone (PNE) and propanal (PNL) over the H-TON catalyst..... | 47 |

LIST OF FIGURES

| Figure | | Page |
|--------|--|------|
| 1.1 | Geometries for (a) SiO ₄ tetrahedral and (b) AlO ₄ /SiO ₄ tetrahedral sharing oxygen vertex..... | 2 |
| 1.2 | Representation of (a) Lewis acid and (b) Brønsted acid in zeolites... | 3 |
| 1.3 | The Structure of ZSM-5 zeolite and tetrahedral (T) positions..... | 4 |
| 1.4 | The structure of MOR zeolite and tetrahedral (T) positions..... | 5 |
| 1.5 | The structure of TON zeolite and tetrahedral (T) positions..... | 6 |
| 1.6 | Dehydration of 1,2-propanediol to propanone and propanal over zeolite catalysts | 8 |
| 2.1 | Schematic illustration of reaction path..... | 15 |
| 3.1 | Ball atoms on the (a) The 52T cluster of H-ZSM-5 modeled as 5T (O ₃ Si-O-SiO ₂ -(OH)-AlO ₂ -O-SiO ₂ -O-SiO ₃) cluster (b) 68T cluster of H-MOR modeled as (O ₃ Si-O-SiO ₂ -(OH)-AlO ₂ -O-SiO ₂ -O-SiO ₃) cluster (c) 56T cluster of H-TON catalysts modeled as (O ₃ Si-(O-SiO ₂) ₂ -(OH)-AlO ₂ -(O-SiO ₂) ₂ -O-Si-O ₃) cluster are treated as high level and the rest of the molecule treated as low level in the two-layered ONIOM(B3LYP/6-31+G(d,p):AM1) method..... | 23 |
| 4.1 | The B3LYP/6-31+G(d,p)-optimized structures of reactant (a) C ₃ H ₈ O ₂ and products (b) CH ₃ COCH ₃ and (c) C ₂ H ₅ CHO | 25 |
| 4.2 | The ONIOM(B3LYP/6-31+G(d,p):AM1)-optimized structures of the (a) 52T cluster of H-ZSM-5, (b) 68T cluster of H-MOR and (c) 56T cluster of H-TON catalysts. Bond distances are in Å..... | 26 |
| 4.3 | The ONIOM(B3LYP/6-31+G(d,p):AM1)-optimized structures of H-ZSM-5 catalyst and its interaction configurations in reaction pathway for 1,2-propanediol (PG) conversion to propanone (PNE). Bond distances are in Å..... | 28 |

| Figure | Page |
|--|-------------|
| 4.4 The ONIOM(B3LYP/6-31+G(d,p):AM1)-optimized structures of H-ZSM-5 catalyst and its interaction configurations in reaction pathway for 1,2-propanediol (PG) conversion to propanal (PNL). Bond distances are in Å..... | 29 |
| 4.5 Potential energy profiles for (a) 1,2-propanediol (PG) conversion to propanone (PNE) and (b) 1,2-propanediol (PG) conversion to propanal (PNL) over the H-ZSM-5 catalyst. Bond distances are in Å..... | 31 |
| 4.6 The ONIOM(B3LYP/6-31+G(d,p):AM1)-optimized structures of H-MOR catalyst and its interaction configurations in reaction pathway for 1,2-propanediol (PG) conversion to propanone (PNE). Bond distances are in Å..... | 35 |
| 4.7 The ONIOM(B3LYP/6-31+G(d,p):AM1)-optimized structures of H-MOR catalyst and its interaction configurations in reaction pathway for 1,2-propanediol (PG) conversion to propanal (PNL). Bond distances are in Å..... | 36 |
| 4.8 Potential energy profiles for (a) 1,2-propanediol (PG) conversion to propanone (PNE) and (b) 1,2-propanediol (PG) conversion to (PNL) over the H-MOR catalyst. Bond distances are in Å..... | 38 |
| 4.9 The ONIOM(B3LYP/6-31+G(d,p):AM1)-optimized structures of H-TON catalyst and its interaction configurations in reaction pathway for 1,2-propanediol (PG) conversion to propanone (PNE). Bond distances are in Å..... | 42 |
| 4.10 The ONIOM(B3LYP/6-31+G(d,p):AM1)-optimized structures of H-TON catalyst and its interaction configurations in reaction | |

| | |
|--|----|
| pathway for 1,2-propanediol (PG) conversion to propanal (PNL). Bond distances are in Å..... | 43 |
|--|----|

| Figure | | Page |
|---------------|--|-------------|
| 4.11 | Potential energy profiles for (a) 1,2-propanediol (PG) conversion to propanone (PNE) and (b) 1,2-propanediol (PG) conversion to propanal (PNL) over the H-TON catalyst. Bond distances are in Å. | 45 |

LIST OF ABBREVIATIONS AND SYMBOLS

| | |
|-------------|---------------------------------------|
| Å | Angstrom |
| B3LYP | Beck 3 Lee–Yang–Parr |
| E | Energy |
| G | Gibb free energy |
| H | Enthalpy |
| S | Entropy |
| DFT | Density functional theory |
| h | Plank's constant |
| \hat{H} | Hamiltonian operator |
| HF | Hartree–Fock |
| LCAO | Linear combination of atomic orbitals |
| MO | Molecular orbital |
| TS | Transition state |
| T | Absolute temperature |
| Ψ | Wave function |
| κ | Kappa |
| STO | Slater type orbital |
| Ψ | Wave function |
| k_B | Boltzman's constant |
| ρ | Electron density |
| q_{total} | Total partition function |
| q_{rot} | Rotation partition function |
| q_{vib} | Vibration partition function |
| q_{tran} | Translation partition function |
| q_{elect} | Electronic partition function |
| k | Rate constant |
| R | Gas constant |
| ν_i | Image frequency |

CHAPTER I

INTRODUCTION

1.1 Background

In the process of biodiesel production a large quantity of glycerol is produced as a by-product, the biodiesel derived glycerol tends to be feedstock for the production 1,2-propanediol by hydrogenolysis. 1,2-propanediol is used to produce propanal and propanone using acid catalysts. Propanal (or propionaldehyde) is used as important chemical reactant in preparation of final products such as paints, rubbers, pesticides and plastic. Propanal compound is produced by petroleum-derived processes such as the propylene oxide isomerization [1], acrolein hydrogenation [2] and ethylene hydroformylation [3]. Propanone (or acetone) is used as important solvent to prepare drugs, fibers and plastics. Propanone compound is produced by petroleum-derived processes such as the propylene oxide isomerization [1], direct extractions from vegetation [4–5] and propane oxidation and other alkanes with a resemble structure [6]. Due to solid acids such as zeolites catalysts have been used for dehydration of alcohols i.e. ethanol and methanol [7–10]. They can be used for dehydration of 1,2-propanediol to produce propanal and propanone.

1.2 Zeolites

Zeolites are microporous crystalline aluminosilicate materials with well-defined structures and balancing cations are generally of alkali and alkaline earth metals. Over 190 different types of synthetic and natural zeolites [11] have been found. Structures of zeolites consist of SiO_4 and AlO_4 tetrahedral which are linked to one another by means of exchange of electrons of the oxygen as shown in Figure 1.1.

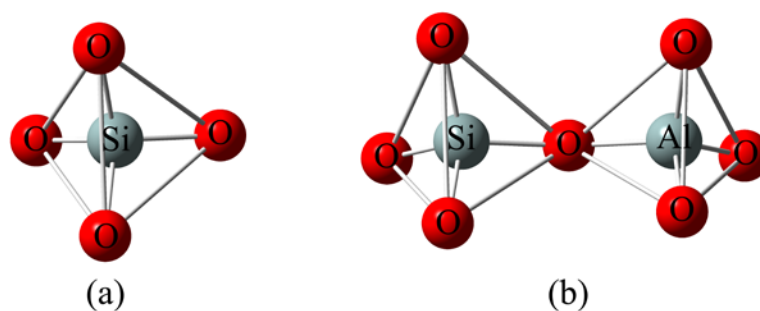


Figure 1.1 Geometries for (a) SiO_4 tetrahedral and (b) $\text{AlO}_4/\text{SiO}_4$ tetrahedral sharing oxygen vertex.

As Al sites in zeolite framework have negative charge and neutralized by charge equivalence framework cations, aluminium atoms in zeolite framework known as silica and aluminium ratio are indicator of acidity.

1.2.1 Acidity of zeolites

Acidic of Brønsted acid sites [12, 13] zeolites were studied using various techniques [14–17]. Lewis and Brønsted acid sites in H-ZSM-5 catalysts studied by means of ^{27}Al double double-quantum magic-angle spinning (DQ-MAS) NMR and ^1H [18] spectroscopic methods. Brønsted acid sites in H-MOR catalysts were investigated by means of Solid-State MAS NMR spectroscopy [19]. Acid sites in H-TON catalyst were studied by deployment of Bellamy-Hallam-William (BHW) plots [20].

The replacement of the Si by Al requires additional positive charge such as proton (H^+) in order to balance the negative charge of the framework. Proton in zeolites is able to release onto any species that can receive proton. The acidity is caused by the proton in zeolites. The term acidity of zeolites mostly describe by Brønsted and Lewis acid as shown in Figure 1.2

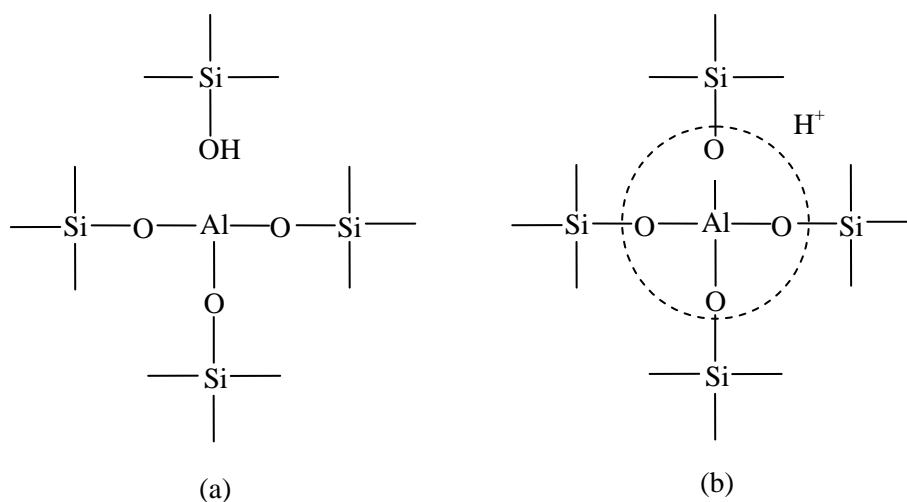


Figure 1.2 Representation of (a) Lewis acid and (b) Brønsted acid in zeolites [21].

1.2.2 ZSM-5 zeolite

ZSM-5 (Zeolite Socony Mobil Number five or MFI topology) is a medium pore, a high-silica zeolite which was discovered by Mobil Oil Company in 1972. It is constructed by 5- and 10-membered rings building units. One is straight channels with dimensions of $5.3 \text{ \AA} \times 5.6 \text{ \AA}$ in diameter and the other channel is sinusoidal with $3.4 \text{ \AA} \times 4.8 \text{ \AA}$ in diameter. The ZSM-5 consists of 12 crystallography nonequivalent tetrahedral positive charge sites (T1- T12) [21]. T1, T2, T3 and T12 are shown in Figure 1.3. Chatterjee and co-worker have chosen T12 site as a possible location of Al substitutions [22, 23].

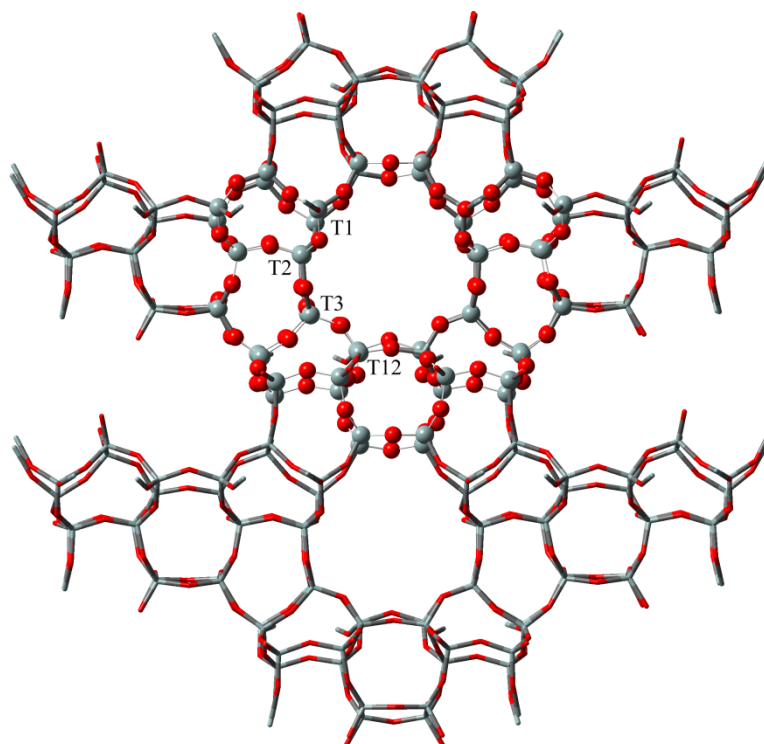


Figure 1.3 The Structure of ZSM-5 zeolite and tetrahedral (T) positions.

1.2.3 MOR zeolite

MOR (Mordenite) zeolite is large-pore, a silica-rich zeolite which is composed of two channels. One is main channel consists of 12-membered ring with dimensions of $6.7 \text{ \AA} \times 7.0 \text{ \AA}$ in diameter and the other channel is side pocket consists of 8-membered ring with $3.4 \text{ \AA} \times 4.8 \text{ \AA}$ in diameter vertical to the main channel. It consists of four crystallographic nonequivalent tetrahedral positive charge sites (T1–T4) as shown in Figure 1.4. Yuan and co-worker have studied the replacement of Al in MOR and proposed that the T2 position in the MOR favors replacement by Al atoms [24].

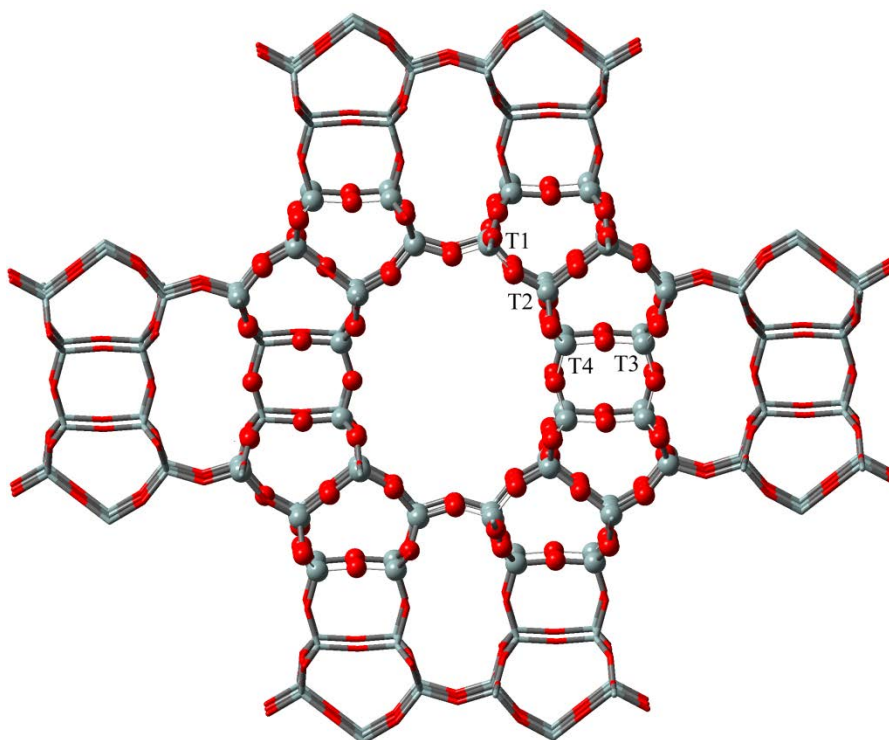


Figure 1.4 The structure of MOR zeolite and tetrahedral (T) positions.

1.2.4 TON zeolite

TON (Theta-1) is uni-dimensional medium pore, high-silica zeolite which consists of 10-membered ring with dimensions of $4.5 \text{ \AA} \times 5.5 \text{ \AA}$ in diameter. [25]. TON zeolite consists of 10-membered ring and four crystallography nonequivalent tetrahedral positive charge sites (T1-T4) as shown in Figure 1.5. Mirosław and co-worker have studied the replacement of Al and thermal stability in TON and proposed that the T3 position in the TON favors replacement by Al atoms [26].

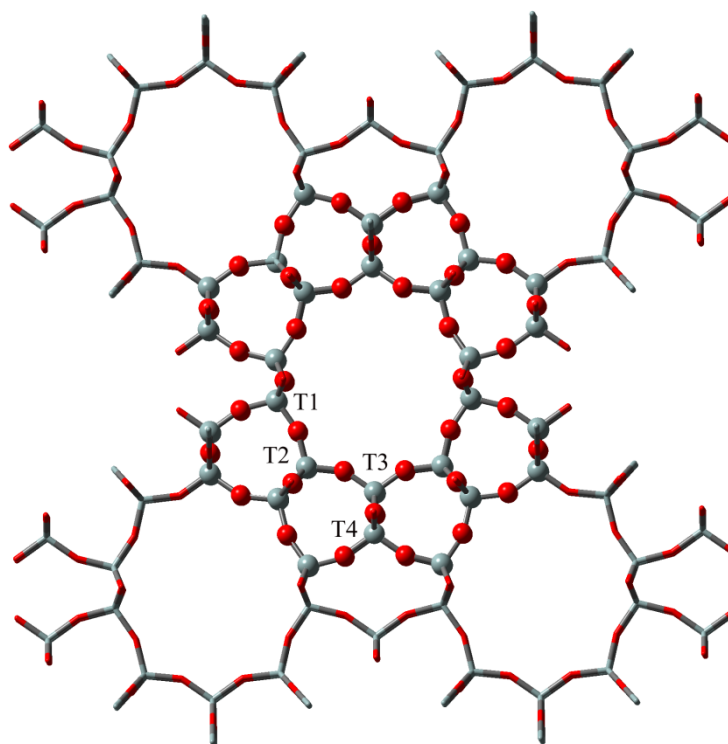


Figure 1.5 The structure of TON zeolite and tetrahedral (T) positions.

1.3 Dehydration of 1,2-propanediol

Dehydration of 1,2-propanediol as known as reaction that can be achieved over acid catalysts via elimination has been proposed in Figure 1.6. For conversion of 1,2-propanediol to propanone, protonation of two hydroxyl groups and rearrangement is able to produce three reactive carbenium intermediates which consist of four reaction steps and conversion of 1,2-propanediol to propanal, protonation of two hydroxyl groups and rearrangement is able to produce two reactive carbenium intermediates consist of three reaction steps [27].

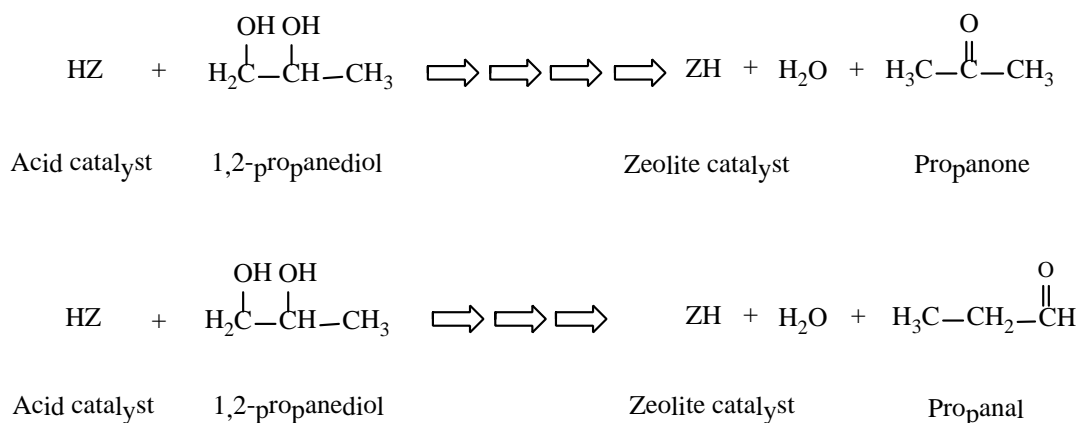


Figure 1.6 Dehydration of 1,2-propanediol to propanone and propanal over zeolite catalysts [27].

Dehydration of 1,2-propanediol can be made over solid acid catalysts [28, 29]. 1,2-propanediol is able to propanone and propanal on solid acid catalysts. Despite dehydration of 1,2-propanediol to propanal and propanone over zeolite catalysts including H-ZSM-5, H-MOR and H-TON catalysts were studied by experiments. No obvious mechanism of these reactions has been reported.

1.4 Objectives

To rationalize and more understanding on the experiments of conversion reaction of ethanol to ethylene, the aim of this work is therefore study of the reaction mechanisms of dehydration of 1,2-propanediol to propanone and propanal over H-ZSM-5, H-MOR and H-TON catalysts using theoretical calculations. Thermodynamic properties, reactions energies, rate and equilibrium constants of dehydration of 1,2-propanediol to propanone and propanal over the H-ZSM-5, H-MOR and H-TON catalysts have been determined using quantum chemical calculations with the ONIOM approach.

CHAPTER II

THEORIES

Theories are used in computational chemistry for description of the structures and interaction between molecules. There are two theories namely quantum mechanics (QM) and molecular mechanics (MM). QM methods, semi-empirical and density functional theory (DFT) methods and their hybrid method have been used in calculations of this work.

2.1 Quantum mechanics method

Quantum mechanics method (QM) is the mathematical description of the behavior of electrons in molecules and can predict properties of molecule or an individual atom. In practice, the QM equations have been resolved accurately for one electron system. A assembly of methods has been developed for approximation for multiple electron systems. The postulate of basic principle of QM is the presence function of coordinate so-called wave function ψ that comprises all probable data about a system [30]. Formulation of QM has been devised by Heisenberg and Schrödinger which are two equivalent formulations applied to computational chemistry.

2.2 Semi-empirical method

Semi-empirical method is simplified forms of Hartree-Fock method with empirical corrections to improve performance. The parameters of semi-empirical computation are derived from experimental data. The most commonly used methods are PM3, MNDO and AM1. The parameterization for PM3, MNDO and AM1 is achieved such that the calculated energies are expressed as heats of formations instead of total energies [31].

2.3 Ab initio method

Ab initio methods are the integral associated with Schrödinger equation. A Hartree–Fock (HF) calculation is the most common type of ab initio calculation, which the primary estimate is the central field calculation. This gives the average effect of the repulsion, but not the explicit repulsion interaction. This is a variational calculation, meaning that the approximate energies calculated are all equal to or greater than the exact energy [32].

2.4 Density functional theory (DFT) method

Density functional theory (DFT) methods are created by theorem of Hohenburg and Kohn. The energy of a molecule is determined from the electron density instead of a wave function. The electron density is expressed as a linear combination of basis functions similar in mathematical form to HF orbitals. DFT methods are used to search for functional relating the electron density with energy.

2.4.1 Kohn–Sham energy

In the Kohn–Sham (KS) formulation of DFT, the energy of system consists of the similar Coulomb part, nuclear and core. The energy of the system, E is written as below:

$$E = E^{Coulomb} + E^{nuclear} + E^{core} + E_{XC}[\rho] \quad (2.1)$$

where $E^{Coulomb}$ is the energy of repulsion between the electrons, $E^{nuclear}$ is the energy of repulsion between the nuclei for a given nuclear configuration, E^{core} is the energy of nucleus with single electron, $E_{XC}[\rho]$ is in terms of function of the electron density, matrix $\rho(r)$. The functional E_{XC} have the form:

$$E_{XC} = \int \rho(r) \varepsilon_{XC}[\rho(r)] dr \quad (2.2)$$

where $\varepsilon_{xc}[\rho(r)]$ is the term of exchange–correlation energy per electron in a homogeneous electron gas of constant density. The Kohn–Sham orbitals ψ_i are used to determine the electron density matrix $\rho(r)$, for a system by N electrons is written as below:

$$\rho(r) = \sum_{i=1}^N |\psi_i|^2 \quad (2.3)$$

2.4.2 Kohn–Sham equations

The Kohn–Sham equations consider the Kohn–Sham wave functions. For a system of N–electrons is written as the following appearance:

$$\left\{ -\frac{1}{2} \nabla_1^2 - \sum_A \frac{Z_A}{r_{A,1}} + \int \frac{\rho(r_2)}{r_{12}} dr_2 + V_{xc}(r_1) \right\} \Psi_1(r_1) = \varepsilon_i \Psi_i(r_1) \quad (2.4)$$

where ε_i is the Kohn–Sham orbital energy, V_{xc} is correlation exchange potential which is exchange–correlation energy derivative functional. The correlation exchange potential is V_{xc} written as below:

$$V_{xc}[\rho] = \frac{\delta E_{xc}[\rho]}{\delta v} \quad (2.5)$$

V_{xc} can be calculated when known E_{xc} [31].

2.4.3 DFT exchange and correlations

For encouragement developing approximate functions in DFT, the functional of E_{xc} is the exchange–correlation energy as the sum of E_x is an exchange–energy functional and E_c is a correlation–energy functional as below:

$$E_{XC} = E_X + E_C \quad (2.6)$$

E_X is determined by the equal method which is used for the exchange energy in Hartree–Fock, but the Kohn–Sham orbitals are replacing the Hartree–Fock orbitals. The replacement of the Kohn–Sham orbitals in the Hartree–Fock orbitals, for a closed–shell molecule is written as:

$$E_X = -\frac{1}{4} \sum_{i=1}^n \sum_{j=1}^n \left\langle \theta_i^{KS}(1) \theta_j^{KS}(2) \left| \frac{1}{r_{12}} \right| \theta_j^{KS}(1) \theta_i^{KS}(2) \right\rangle \quad (2.7)$$

Where θ_i^{KS} is the spatial part of each spin–orbital in position x_1, y_1, z_1 , θ_j^{KS} in position x_2, y_2, z_2 and r_{12} is the distance between points x_1, y_1, z_1 x_2, y_2, z_2 and E_C is determined by the difference between E_X and E_{XC} ; $E_C \equiv E_{XC} - E_X$

2.4.4 Hybrid functions

A hybrid functional is combinations of the formula (2.7) for E_X with gradient–corrected E_X and E_C formulae in equation (2.8).

$$E_{XC}^{GGA} = E_X^{GGA} + E_C^{GGA} \quad (2.8)$$

The term GGA stands for generalized–gradient approximation. The hybrid functional proposed by Becke is written as:

$$E_{XC}^{GGA} = E_X^{GGA} + c_X E_X^{exact} + E_C^{GGA} \quad (2.9)$$

where E_{XC}^{GGA} and E_C^{GGA} are definite GGA functional which contains six and three parameters, c_X is a parameter and E_X^{exact} is E_X of Hartree–Fock definition as given

by (2.7). The common hybrid functional is B3LYP (Beck3LYP) which is determined by:

$$E_{XC}^{B3LYP} = (1 - a_0 - a_x)E_X^{LSDA} + a_0E_X^{exact} + a_xE_x^{B88} + (1 - a_c)E_c^{VWN} + a_cE_c^{LYP} \quad (2.10)$$

where $a_0 = 0.20$, $a_x = 0.72$, and $a_c = 0.81$, E_c^{LYP} is LYP correlation functional, E_x^{B88} is Becke 88 exchange functional, E_c^{VWN} is function of the Vosko–Wilk–Nusair and E_c^{LYDA} is the kind accurate pure LSDA (local–spin–density approximation).

2.5 Basis sets

Basis set is a set of mathematical functions for description of the orbitals in a system, which is expanded by means of linear combination of atomic orbitals (LCAO). The LCAO consists of two types of basis function which usually used in the electronic structure scheming, Slater type orbitals (STO) and Gaussian type orbitals (GTO).

2.5.1 Slater–type orbital (STO)

Slater–type orbital (STO) has the function form:

$$f^{STO}(r) = \left(\frac{\xi^3}{\pi} \right)^{1/2} \exp(-\xi r) \quad (2.11)$$

where ξ is the Slater orbital exponent. For fitting atomic orbitals the STOs are interesting but for more two atoms STOs are complications in estimating the required integrals. To solve these problems, Gaussian type orbitals (GTO) are usually substituted by STO.

2.5.2 Gaussian type orbitals (GTO)

Gaussian type orbitals (GTO) have the function form:

$$f^{GTO}(r) = \left(\frac{2\alpha}{\pi}\right)^{3/4} \exp(-\alpha r^2) \quad (2.12)$$

where α is GTO exponent. The first derivative of GTO when r be likely zero is void, on the other hand the non void value succeeded by some STO.

2.5.3 Minimal basis sets

Basis set allocates a set of basis functions to every atom in a molecule to approximate its orbitals. Minimal basis sets contain the minimum number of basis set which are used for each atom. Minimal basis sets use atomic type orbitals of which size and fixed.

2.5.4 Split the valence basis sets

The split valence basis sets are orbitals of which every valence are splitted into two parts, an inner-shell and outer-shell. Split valence basis sets have two or more sizes of basis function for each valence orbital.

2.5.5 Polarization basis sets

Polarization basis sets are method to carry on the more atomic orbital functions in the calculation to improve the outcome. The Polarization basis sets are to adding p functions on hydrogen and d functions on heavy atoms which permit the replacement of the electron density from the nuclear site.

2.5.6 Diffuse functions

Diffuse functions are function using a large size of s- and p-type functions. These functions are significant for system of which electrons are far away from nucleus. The 6-31+G(d) is the 6-31G(d) basis set which diffuse function are added to heavy atoms in computed molecule.

2.6 The ONIOM method

ONIOM (our own n-layered integrated molecular orbital and molecular mechanic) method is one of the most popular hybrid method to treat on molecular systems. ONIOM method is a simple linear extrapolation procedure which allows the ONIOM method to be extended to two-layer and three-layer ONIOM. Hybrid QM/QM method such as ONIOM (QM1:QM2) is a method which QM1 and QM2 are used as high and low levels of theory. The ONIOM method works by approximating the energy of the Real System (R) as a combination of the energies computed by less expensive methods.

2.7 Transition state theory and rate constant

Transition state theory (TST) provides an approach to explain the temperature and concentration dependence of the rate law. TST is defined as the maximum value on the minimum energy path (MEP) of the potential energy surface which is connection between reactant and product. In chemistry, TST is a conception of chemical reactions involving rearrangement of species as transition state (TS). TS is the configuration which divides the reactant and product parts of surface as shown in Figure 2.1.

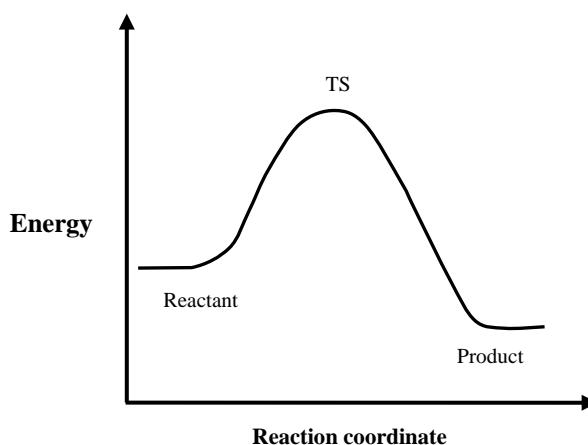


Figure 2.1 Schematic illustration of reaction path.

2.7.1 Rate constant and Boltzman distribution

TST assumes equilibrium energy distribution among all possible quantum states along the reaction coordinates. The probability of finding a molecule in a given quantum state is proportional to Boltzman distribution, $e^{-\Delta E/k_B T}$. Rate constant can be determined using Eyring equation as written:

$$k = \frac{k_B T}{h c^0} e^{-\Delta^\ddagger G / RT} \quad (2.13)$$

$\Delta^\ddagger G$ is the Gibbs free energy difference between the TS and reactant, T is absolute temperature and k_B is Boltzmann's constant. c^0 is concentration factor. The equilibrium constant for a reaction can be computed from the free energy change between the reactant and product.

$$K_{eq} = e^{-\Delta G_0 / RT} \quad (2.14)$$

The Gibbs free energy (G) is defined as a thermodynamic equation, $G = H - TS$.

2.7.2 Rate constant with tunneling corrections

Tunneling corrections can be computed using the Wigner method [33]. The Wigner method is a simple, zeroth-order tunneling approximation and only depends on the curvature at transition state. Reaction rate coefficients can be obtained using the following equation.

$$k = \kappa \left[\frac{k_B T}{h} \right] \left[\frac{Q_{TS}}{Q_{Complex}} \right] e^{-\Delta^\ddagger E / RT} \quad (2.15)$$

where tunneling factor, $\kappa = 1 + (1/24)(h\nu_i c / k_B T)^2$, k_B is Boltzman constant, T is absolute temperature, Q_{TS} and $Q_{Complex}$ are the partition functions of transition state and complex, respectively, h is Plank constant, c is speed of light and ν_i is imaginary frequency of transition state.

2.7.3 Partition functions

For determination of the thermal contributions to the enthalpies and entropies of a molecule, its partition function, q must be first determined at a particular temperature and q is a measure of the number of accessible to the molecule i.e. translational, rotational, vibrational and electronic states.

As the translational (T), rotational (R), vibrational (V) and electronic (E) modes of the system can be separated, the energy of each level (E_i) can therefore be separated into T , R , V and E contributions as

$$E = E_i^T + E_i^R + E_i^V + E_i^E \quad (2.16)$$

While the translational modes are independent from the rest, the separations of other modes are based on an approximation, in particular the Bohn–Oppenheimer approximation for electronic and vibrational motion and the rigid rotor approximation. Within these approximations, the total molecular partition function

can be factorized into contributions as translational (q_{trans}), vibrational (q_{vib}), rotational (q_{rot}) and electronic (q_{elect}) partition functions:

$$q = q_{trans} q_{vib} q_{rot} q_{elect} \quad (2.17)$$

2.7.3.1 Translation partition function

For bimolecular reactions, the translational partition functions may be simplified as the relative translational partition in per unit volume as:

$$q_{trans} = \frac{V}{\Lambda^3} \quad (2.18)$$

where

$$\Lambda = h \left(\frac{\beta}{2\pi m} \right)^{1/2} \quad (2.19),$$

h is Planck's constants, m is the mass of the molecule and V is the available volume to it. For a gas phase system, this is the molar volume at the specific temperature and pressure.

2.7.3.2 Rotational partition function

The rotational partition functions of linear and non linear molecules are different terms. For linear molecules

$$q_{rot} = \frac{k_B T}{\sigma h c B} \quad (2.20)$$

and for non linear

$$q_{rot} = \frac{1}{\sigma} \left(\frac{k_B T}{hc} \right)^{3/2} \left(\frac{\pi}{ABC} \right)^{1/2} \quad (2.21)$$

2.7.3.3 Vibrational partition function

The vibrational partition functions are computed quantum mechanically within the harmonic approximation framework. The harmonic oscillator partition function is given by:

$$q_{trans} = \prod_i \frac{1}{1 - e^{-\beta h c \tilde{\nu}_i}} \quad (2.22)$$

where $\tilde{\nu}_i$ is the vibrational frequency in cm^{-1} for mode i . The product is over all vibrational modes.

2.7.3.4 Electronic partition function

As an adiabatic potential energy surface for the electronic partition function is assumed, the electronic degeneracies along the MEP are assumed as same as at the transition state. The electronic partition function can therefore be written as

$$q_{elect} = \omega_{e1} + \omega_{e1} \exp(-\beta \Delta \varepsilon_{12}) + \dots \quad (2.23)$$

where $\Delta \varepsilon_{12}$ is the energy of the j^{th} electronic level relative to the ground state and ω_{e1} is the corresponding degeneracy.

2.8 Molecular vibrational frequencies

The total molecular energy E is approximate to be the sum of translation, rotational, vibrational, and electronic energies. As the harmonic oscillator for system is assumed, the vibrational energy of an N -atom molecule is the sum of $3N-6$ and $3N-5$ normal mode vibrational energies for a non-linear and a linear molecule, respectively [34]:

$$E_{vib} \approx \sum_{k=1}^{3N-6} \left(\nu_k + \frac{1}{2} \right) h\nu_k \quad (2.24)$$

where ν_k is the harmonic vibrational frequency for the k^{th} normal mode and ν_k is each vibrational quantum number which is independent of the value of the order vibrational quantum numbers.

The harmonic vibrational frequencies of a molecule are (i) solving the electronic Schrödinger equation $(\hat{H}_{el} + V_{NN})\psi_{el} = U\psi_{el}$ to find the equilibrium geometry of the molecule, (ii) computing the set of second derivatives $(\partial^2 U / \partial X_i \partial X_j)_e$ of the molecular electronic energy U with respect to the $3N$ nuclear Cartesian coordinates of a system with origin at the center of mass, (iii) the mass-weighted force-constant matrix elements is formed as:

$$F_{ij} = \frac{1}{(m_i m_j)^{1/2}} \left(\frac{\partial^2 U}{\partial X_i \partial X_j} \right)_e \quad (2.25)$$

where i and j each run from 1 to $3N$ and m_i is the mass of the atom corresponding to coordinate X_i and (iv) solving the following set of $3N$ linear equations in $3N$ unknowns

$$\sum_{j=1}^{3N} (F_{ij} - \delta_{ij} \lambda_k) l_{jk} = 0 \quad i = 1, 2, \dots, 3N \quad (2.26)$$

where δ_{ij} is the Kronecker delta. λ_k and the l_{jk} 's are unknown parameters of which significance will be seen shortly. As this set of homogeneous equations has a nontrivial solution, the coefficient determinant must vanish then:

$$\det(F_{ij} - \delta_{ij} \lambda_k) = 0 \quad (2.27)$$

Due to this coefficient determinant is of order $3N$, its expansion gives a polynomial of which whose highest power of λ_k is λ_k^{3N} . The molecular harmonic vibrational frequencies can be computed from equation:

$$\nu_k = \lambda_k^{1/2} / 2\pi \quad (2.28)$$

2.9 Thermochemistry

In general definition, the enthalpies ($\Delta_f H^\circ (298 \text{ K})$) of reaction at 298 K can be calculated using the following equation [35].

$$\Delta_r H^\circ (298 \text{ K}) = \sum_{\text{products}} \Delta_f H^\circ_{\text{prod}} (298 \text{ K}) - \sum_{\text{reactants}} \Delta_f H^\circ_{\text{react}} (298 \text{ K}) \quad (2.29)$$

The Gibbs free energy ($\Delta_f G^\circ (298 \text{ K})$) of reaction can be computed using the following equation:

$$\Delta_f G^\circ (298 \text{ K}) = \Delta_f H^\circ (298 \text{ K}) - T(S^\circ(M, 298 \text{ K}) - \sum S^\circ(X, 298 \text{ K})) \quad (2.30)$$

where M stands for the molecule and X represents each element which makes up M , and x will be the number of atoms of X in M .

Atomization energy of the molecule, $\sum D_0(M)$ is a function of the total energies of the molecule $\sum \varepsilon_0(M)$, the zero-point energy of the molecule ($\varepsilon_{ZPE}(M)$) as shown below:

$$\sum D_0(M) = \sum_{\text{atoms}} x\varepsilon_0(X) - \varepsilon_0(M) - \varepsilon_{ZPE}(M) \quad (2.31)$$

Finally, $\Delta_f H^\circ(298 K)$ and $\Delta_f G^\circ(298 K)$ can be obtained as following calculations:

1. Calculate $\Delta_f H^\circ(M, 0 K)$ for each molecule:

$$\begin{aligned}\Delta_f H^\circ(M, 0 K) &= \sum_{atoms} x \Delta_f H^\circ(X, 0 K) - \sum D_0(M) \\ &= \sum_{atoms} x \Delta_f H^\circ(X, 0 K) - (\sum_{atoms} x \varepsilon_0(X) - \varepsilon_0(M))\end{aligned}\quad (2.32)$$

2. Calculate $\Delta_f H^\circ(M, 298 K)$ for each molecule:

$$\begin{aligned}\Delta_f H^\circ(M, 298 K) &= \Delta_f H^\circ(M, 0 K) + (H_M^\circ(298 K) - H_M^\circ(0 K)) \\ &\quad - \sum_{atoms} x (H_X^\circ(298 K) - H_X^\circ(0 K))\end{aligned}\quad (2.33)$$

3. Calculate $\Delta_f G^\circ(M, 298 K)$ for each molecule:

$$\Delta_f G^\circ(M, 298 K) = \Delta_f H^\circ(298 K) + 298.15(S^\circ(M, 298 K) - \sum S^\circ(X, 298 K)) \quad (2.34)$$

where $(\Delta_f H^\circ(X, 0 K))$ [31] is heats of formation of the atoms at 0K, $H_x^\circ(298 K) - H_x^\circ(0 K)$ is enthalpy corrections of the atomic elements, $H_M^\circ(298 K) - H_M^\circ(0 K)$ is enthalpy correction for the molecule, $S_x^\circ(298 K)$ is entropy for the atoms and $S_M^\circ(298 K)$ is entropy for the molecule.

CHAPTER III

COMPUTATIONAL DETAILS

Due to the two-layered ONIOM(MO:MO) approach [36, 37], ball atoms as 5T ($\text{O}_3\text{Si}-\text{O}-\text{SiO}_2-(\text{OH})-\text{AlO}_2-\text{O}-\text{SiO}_2-\text{O}-\text{SiO}_3$), 5T ($\text{O}_3\text{Si}-\text{O}-\text{SiO}_2-(\text{OH})-\text{AlO}_2-\text{O}-\text{SiO}_2-\text{O}-\text{SiO}_3$) and 7T $\text{O}_3\text{Si}-(\text{O}-\text{SiO}_2)_2-(\text{OH})-\text{AlO}_2-(\text{O}-\text{SiO}_2)_2-\text{O}-\text{SiO}_3$ clusters on the H-ZSM-5, modeled as 52T ($\text{H}_{40}\text{Si}_{51}(\text{HO})\text{AlO}_{83}$), H-MOR modeled 68T ($\text{H}_{60}\text{Si}_{67}(\text{HO})\text{AlO}_{105}$) and H-TON modeled as 56T ($\text{H}_{56}\text{Si}_{55}(\text{HO})\text{AlO}_{83}$) clusters as shown in Figure 4.1 and all interaction species are treated as high level (B3LYP/6-31+G(d,p) level of theory [38–40] and the rest of the molecule treated as low level (AM1 level [41]).

3.1. Cluster models for the H-ZSM-5, H-MOR and H-TON

The structures of 52T ($\text{H}_{40}\text{Si}_{51}(\text{HO})\text{AlO}_{83}$), 68T ($\text{H}_{60}\text{Si}_{67}(\text{HO})\text{AlO}_{105}$) and 56T ($\text{H}_{56}\text{Si}_{55}(\text{HO})\text{AlO}_{83}$) clusters respectively modeled for H-ZSM-5, H-MOR and H-TON zeolites were constructed from the idealized infinite ZSM-5 [42], MOR [43] and TON [44] crystal lattice structures, respectively. The crystal lattice structures of ZSM-5, MOR and TON respectively cut as 52T, 68T and 56T were decorated as following treatment. The dangling bonds of 52T ZSM-5, 68T MOR and 56T TON clusters were saturated with hydrogen atoms, one silicon atom located at the crystallographic positions T12, T2 and T3 were substituted by one aluminum atom, respectively. The complete clusters for H-ZSM-5, H-MOR and H-TON catalysts were obtained by bonding one proton to oxygen atom which bridges between the T12-, T2- and T3-aluminum atom of the ZSM-5, MOR and TON clusters, respectively. The 52T cluster of H-ZSM-5, 68T cluster of H-MOR and 56T cluster of H-TON catalysts and their clusters modeled as 5T ($\text{O}_3\text{Si}-\text{O}-\text{SiO}_2-(\text{OH})-\text{AlO}_2-\text{O}-\text{SiO}_2-\text{O}-\text{SiO}_3$), 5T ($\text{O}_3\text{Si}-\text{O}-\text{SiO}_2-(\text{OH})-\text{AlO}_2-\text{O}-\text{SiO}_2-\text{O}-\text{SiO}_3$) and 7T $\text{O}_3\text{Si}-(\text{O}-\text{SiO}_2)_2-(\text{OH})-\text{AlO}_2-(\text{O}-\text{SiO}_2)_2-\text{O}-\text{SiO}_3$ clusters, respectively and definition of high

and low levels of theory applied in the two-layered ONIOM(B3LYP/6-31+G(d,p):AM1) approach are shown in Figure 3.1.

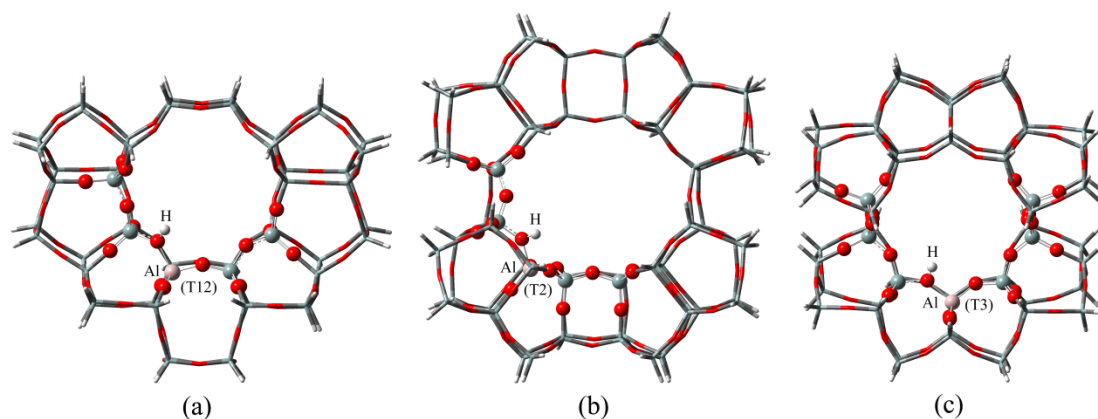


Figure 3.1. Ball atoms on the (a) 52T cluster of H-ZSM-5, (b) 68T cluster of H-MOR and (c) 56T cluster of H-TON catalysts, respectively modeled as 5T ($\text{O}_3\text{Si}-\text{O}-\text{SiO}_2-(\text{OH})-\text{AlO}_2-\text{O}-\text{SiO}_2-\text{O}-\text{SiO}_3$), 5T ($\text{O}_3\text{Si}-\text{O}-\text{SiO}_2-(\text{OH})-\text{AlO}_2-\text{O}-\text{SiO}_2-\text{O}-\text{SiO}_3$) and 7T ($\text{O}_3\text{Si}-(\text{O}-\text{SiO}_2)_2-(\text{OH})-\text{AlO}_2-(\text{O}-\text{SiO}_2)_2-\text{O}-\text{SiO}_3$) clusters are treated as high level and the rest of the molecule treated as low level in the two-layered ONIOM(B3LYP/6-31+G(d,p):AM1) approach.

3.2 Structure optimization and potential energy surface

The ONIOM(B3LYP/6-31+G(d,p):AM1)-optimized structures of transition-state for the reaction steps for 1,2-propanediol dehydration to propanal and to propanone over the H-ZSM-5, H-MOR and H-TON were located using the reaction coordinate method referred to the synchronous transit-guided quasi-newton (STQN) calculation [45] using GAUSSIAN 03 program.

3.3. Thermodynamic properties and formation constants

The standard enthalpy ΔH_{298}° and Gibbs free energy change ΔG_{298}° of all studied reactions have been derived from the zero-point vibrational energy (ZPVE) computed at the ONIOM(B3LYP/6-31+G(d,p):AM1) level of theory. The rate constants $k(T)$ for conversion reactions of the conversion of ethanol to ethylene derived from the transition-state theory were computed from activation energy ($\Delta^{\ddagger}E$) using Eq. (3.1)

$$k(T) = \kappa \frac{k_B T}{h} \frac{Q_{TS}}{Q_{REA}} \exp(-\Delta^{\ddagger}E/RT) \quad (3.1)$$

where k_B is the Boltzmann's constant, h is Plank's constant, T is the absolute temperature, R is the gas constant, and Q_{TS} and Q_{REA} are the partition functions of the transition state and the reactant of reaction step whose values are composed of translational, rotational, and vibrational partition functions. The tunneling coefficient (κ) can be computed with the Wigner method [49–51] as $\kappa = 1 + (1/24) (h\nu_i/k_B T)^2$ where ν_i is the imaginary frequency that accounts for the vibration motion along the reaction path. The pre-exponential factor (A) is defined as $A = (k_B T/h) (Q_{TS}/Q_{REA})$. The equilibrium constant K at 298.15 K and 1 atm is computed using a thermodynamic equation $\Delta G^{\circ} = -RT \ln K$.

CHATER IV

RESULTS AND DISCUSSION

4.1 Optimized structures of zeolite catalysts and involved compounds

The B3LYP/6-31+G(d,p)-optimized structures of reactant and products are shown in Figure 4.1. As the structures H-ZSM-5, H-MOR and H-TON catalysts were respectively modeled as 52T, 68T and 56T clusters, the 52T cluster of H-ZSM-5, 68T cluster of H-MOR and 56T cluster of H-TON structures optimized using ONIOM(B3LYP/6-31+G(d,p):AM1) method were obtained as shown in Figure 4.2.

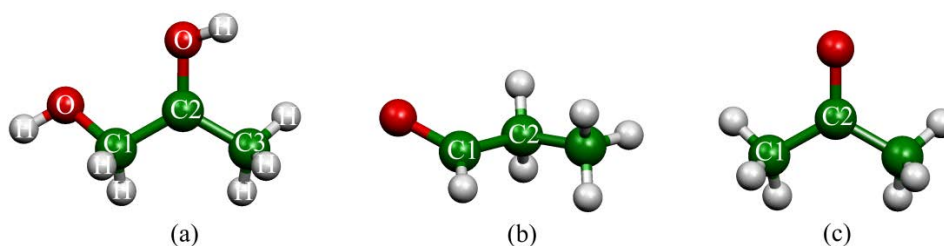


Figure 4.1. The B3LYP/6-31+G(d,p)-optimized structures of reactant (a) 1,2-propanediol and products (b) propanal and (c) propanone.

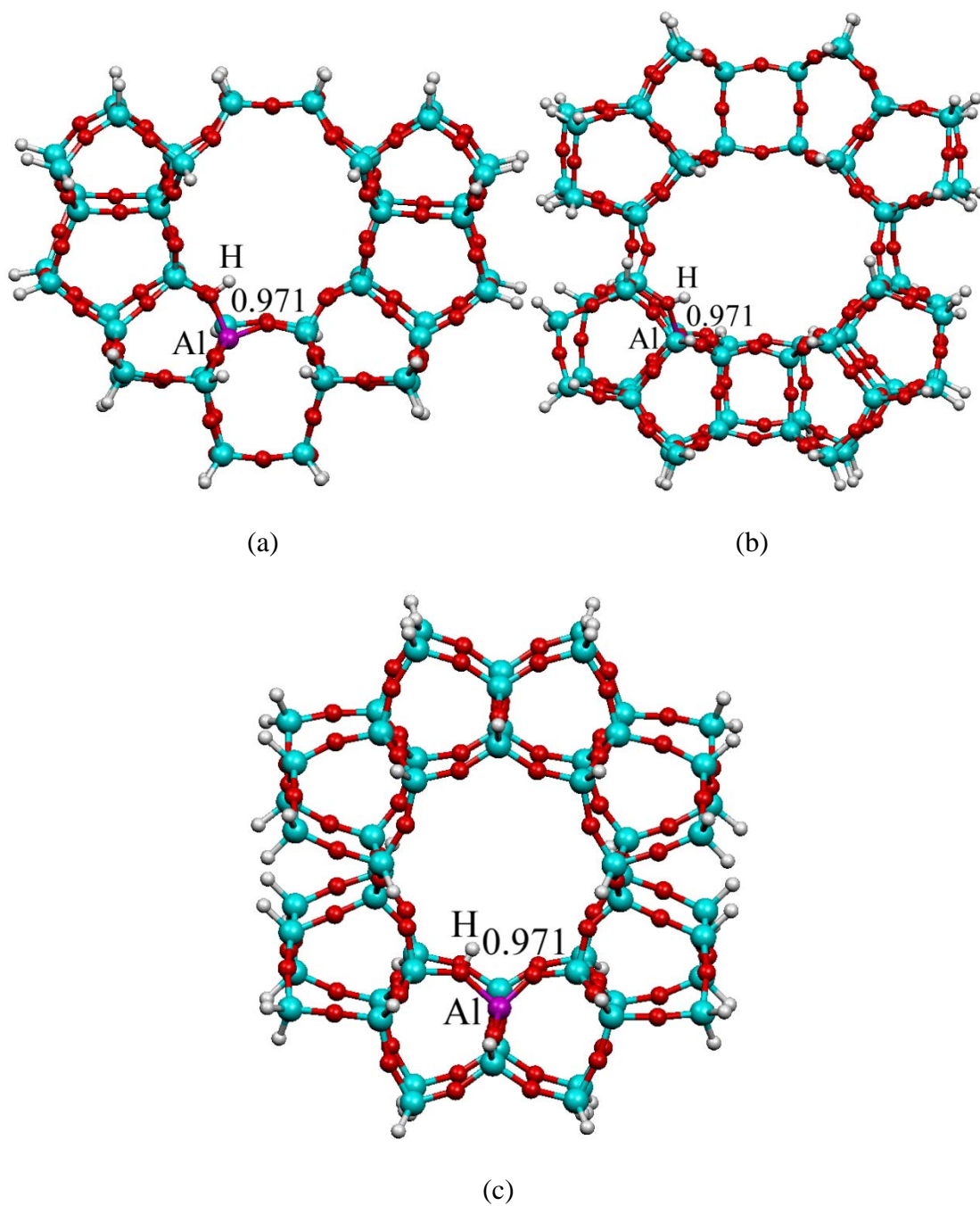


Figure 4.2. The ONIOM(B3LYP/6-31+G(d,p):AM1)-optimized structures of the (a) 52T cluster of H-ZSM-5, (b) 68T cluster of H-MOR and (c) 56T cluster of H-TON catalysts. Bond distances are in Å.

The H–O bond length of the H–ZSM–5 are 0.971 Å for HZ configuration and 0.974 Å for ZH configuration of which stretching vibrations are 3792.6 and 3758.9 cm^{-1} , respectively. These two vibration frequencies are closed to experiments [46]. For the H–O bond length of the H–MOR are 0.971 Å for HZ configuration and 0.978 Å for ZH configuration of which stretching vibrations are 3778.1 and 3690.6 cm^{-1} , respectively. For the H–O bond length of the H–TON are 0.971 Å for HZ configuration and 0.971 Å for ZH configuration of which stretching vibrations are 3789.8 and 3789.5 cm^{-1} , respectively. As it was found that the H–ZSM–5, the H–MOR and H–TON their HZ form is more stable than their ZH by 22.78, 23.08 and 0.31 kcal/mol, the reaction for ZH to HZ is energetically preferred reaction.

4.2 Conversion of 1,2–propanediol over the H–ZSM–5

The reaction mechanism of 1,2–propanediol over the H–ZSM–5 was found to consist of two reaction paths. The first path is the conversion of 1,2–propanediol to propanone and the second path is conversion to propanal as shown in Figures 4.3 and 4.4, respectively. The first reaction path and ONIOM(B3LYP/6–31+G(d,p):AM1)–optimized structures of H–ZSM–5 catalyst as HZ and ZH of which acidic proton bond to oxygen atom bridged between right next two silicon atoms, are shown in Figure 4.3. It shows also the structures of interaction configurations with H–ZSM–5 in reaction pathway for 1,2–propanediol conversion to propanone. The second reaction path and the related ONIOM(B3LYP/6–31+G(d,p):AM1)–optimized structures are shown in Figure 4.4.

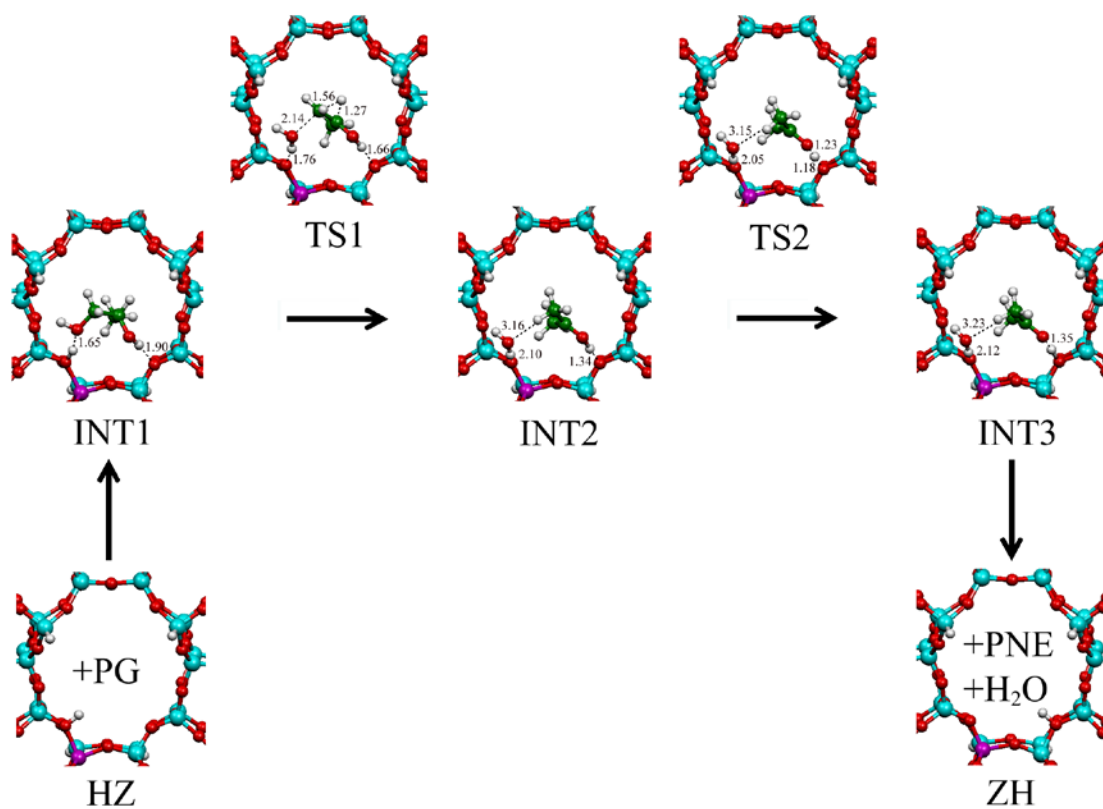


Figure 4.3. The ONIOM(B3LYP/6-31+G(d,p):AM1)-optimized structures of H-ZSM-5 catalyst and its interaction configurations in reaction pathway for 1,2-propanediol (PG) conversion to propanone (PNE). Bond distances are in Å.

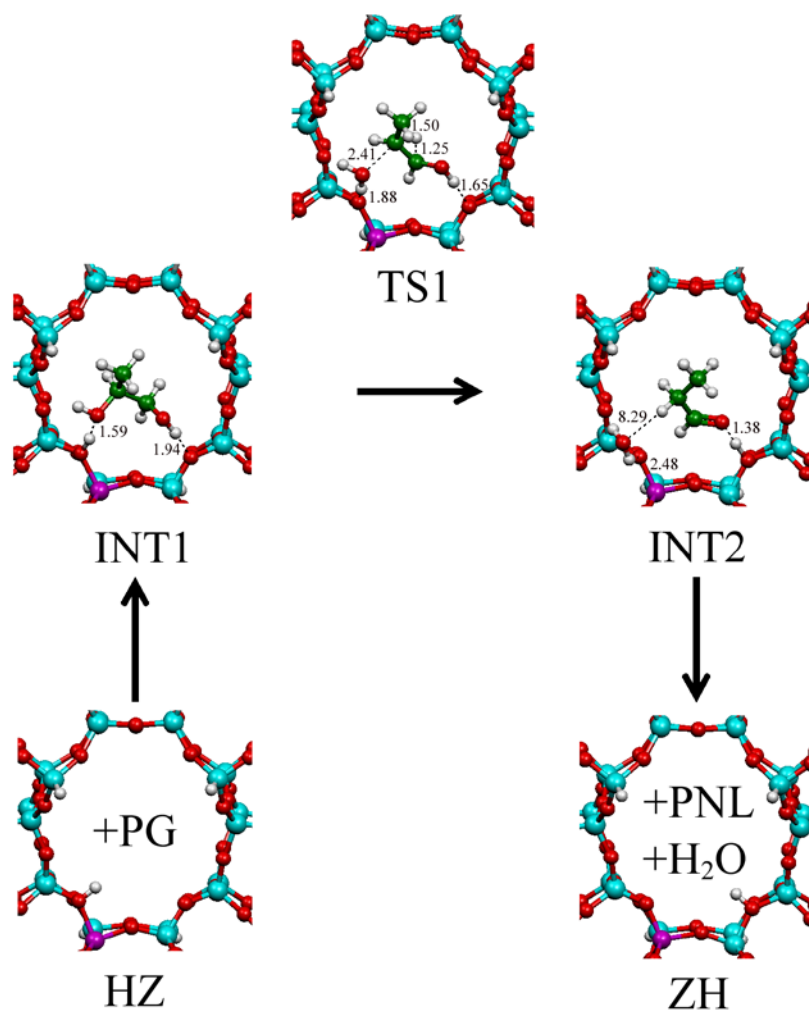


Figure 4.4. The ONIOM(B3LYP/6-31+G(d,p):AM1)-optimized structures of H-ZSM-5 catalyst and its interaction configurations in reaction pathway for 1,2-propanediol (PG) conversion to propanal (PNL). Bond distances are in Å.

Potential energy profiles for 1,2-propanediol conversion to propanone and to propanal over the H-ZSM-5 catalyst are shown in Figure 4.5(a) and (b), respectively. The conversion of 1,2-propanediol conversion to propanone is composed of four reaction steps. The first step, 1,2-propanediol adsorbs onto the H-ZSM-5 by pointing hydroxyl oxygen of hydroxyl group at the 1-position carbon atom toward the acid proton of H-ZSM-5 and pointing hydroxyl hydrogen atom of the other hydroxyl group toward oxygen atom of the H-ZSM-5, shown as INT1 in Figure 4.3. The second step, the intermediate reactant INT1 affords the intermediate INT2 via transition state TS1. One water molecule was formed and bound to H-ZSM-5 oxygen atom. This step is therefore a dehydration step. The hydrogen-bond length, in INT1 (1.90 Å) is longer than that in INT2 (1.34 Å) by 0.56 Å. This means that [H \cdots O] hydrogen-bond in INT2 is stronger than that in INT1 because of the [H \cdots O] in INT2 is a single hydrogen bonding with positive charge. The third step, the intermediate reactant INT2 affords the intermediate INT3 via transition state TS2. This step is the proton transfer process in order to retain the H-ZSM-5 as ZH. The last step is the desorption process of water and propanone as final product.

The conversion of 1,2-propanediol conversion to propanal comprises three reaction steps. The first step, 1,2-propanediol adsorbs onto the H-ZSM-5 by pointing hydroxyl oxygen of hydroxyl group at the 2-position carbon atom toward the acid proton of H-ZSM-5 and pointing hydroxyl hydrogen atom of the other hydroxyl group toward oxygen atom of the H-ZSM-5, shown as INT1 in Fig. 4. The second step (dehydration step), the intermediate reactant INT1 affords the intermediate INT2 via transition state TS1 and one water molecule was formed and bound to H-ZSM-5 oxygen atom. The hydrogen-bond length, in INT1 (1.90 Å) is longer than that in INT2 (1.40 Å) by 0.50 Å. The last step is the desorption process to afford propanal product.

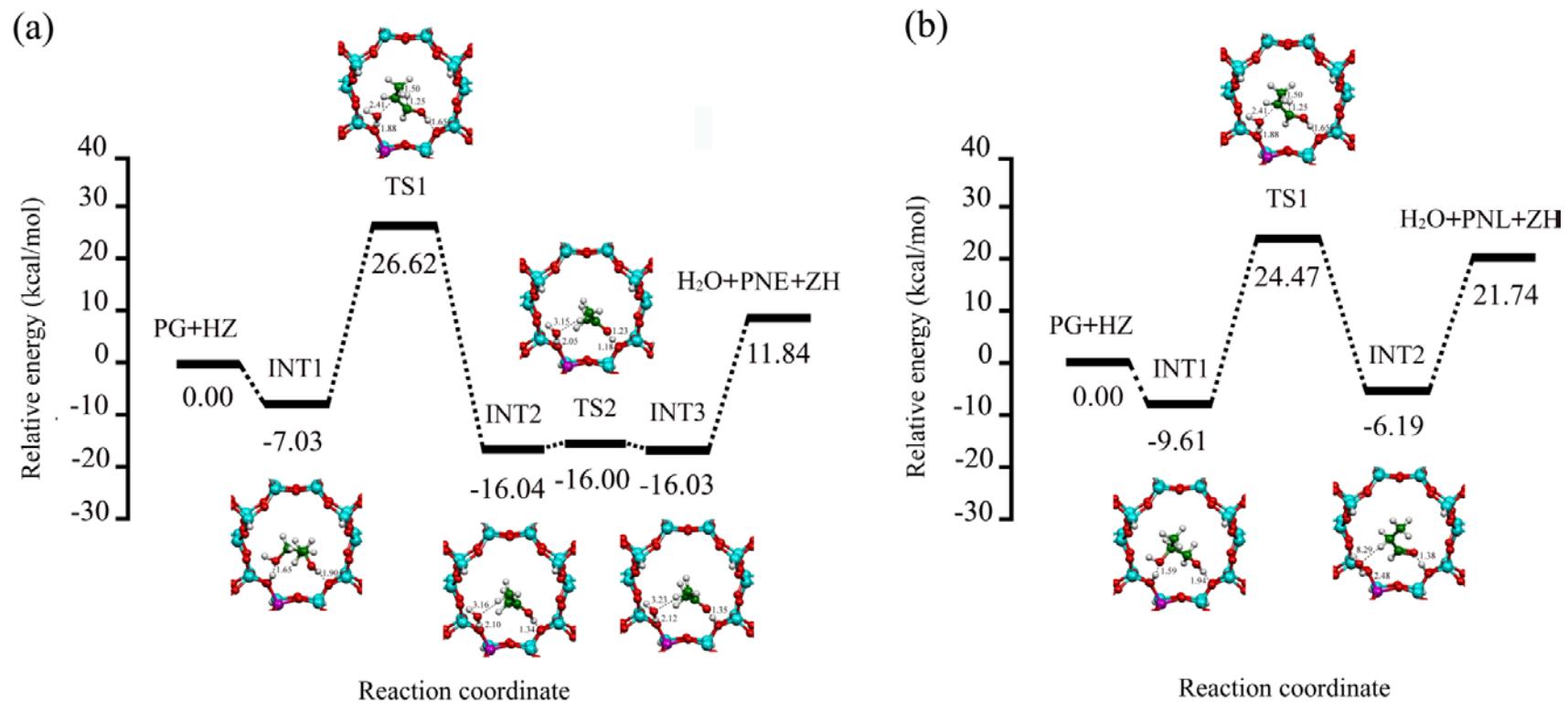


Figure 4.5. Potential energy profiles for (a) 1,2-propanediol (PG) conversion to propanone (PNE) and (b) to (PNL) over the H-ZSM-5 catalyst.

The reaction energies, thermodynamic properties, rate constants and equilibrium constants for conversion reactions of 1,2-propanediol to propanone and propanal over the H-ZSM-5 catalyst are shown in Table 4.1. The rate determining step for the propanone pathway is the second step of which rate constant is $1.21 \times 10^{-12} \text{ s}^{-1}$ and for the propanal pathway is the second step of which rate constant is $4.09 \times 10^{-12} \text{ s}^{-1}$. The over all equilibrium constants for the propanone and propanal pathways are 1.71×10^{-2} and 8.53×10^{-8} , respectively. The overall reaction enthalpies of both pathways are exothermic process.

Table 4.1 Reaction energies, thermodynamic properties, rate constants and equilibrium constants for conversion reactions of 1,2–propanediol (PG) to propanone (PNE) and propanal (PNL) over the H–ZSM–5 catalyst.

| Catalysts/Reactions ^a | $\Delta^\ddagger E$ ^{a,b} | $\Delta^\ddagger G$ ^{a,b} | k_{298} ^c | ΔE ^a | ΔH_{298} ^a | ΔG_{298} ^a | K_{298} |
|-----------------------------------|------------------------------------|------------------------------------|------------------------|-------------------------|-------------------------------|-------------------------------|-----------------------|
| <i>Pathway for Propanone:</i> | | | | | | | |
| PG + HZ → INT1 | – | – | – | –7.03 | –7.03 | 6.12 | 3.29×10^{-5} |
| INT1 → TS1 → INT2 | 33.65 | 33.96 | 1.21×10^{-12} | –9.01 | –8.03 | –10.38 | 4.06×10^7 |
| INT2 → TS2 → INT3 | 0.04 | 0.33 | 3.63×10^{12} | 0.00 | –0.16 | 0.33 | 5.70×10^{-1} |
| INT3 → PNE + H ₂ O +ZH | – | – | – | 27.87 | 28.52 | 6.34 | 2.25×10^{-5} |
| <i>Pathway for Propanal:</i> | | | | | | | |
| PG + HZ → INT1 | – | – | – | –9.51 | –9.61 | 3.94 | 1.30×10^{-3} |
| INT1 → TS1 → INT2 | 33.57 | 33.22 | 4.09×10^{-12} | 2.07 | 3.42 | –0.16 | 1.30×10^0 |
| INT2 → PNL + H ₂ O +ZH | – | – | – | 27.46 | 27.86 | 5.86 | 5.05×10^{-5} |

^a Computed at ONIOM(B3LYP/6–31+G(d,p):AM1) level, in kcal mol^{–1}.

^b Activation energy.

^c In s^{–1}.

4.3 Conversion of 1,2-propanediol over the H-MOR

The reaction mechanism of 1,2-propanediol over the H-MOR was also found to consist of two reaction paths. One is the conversion of 1,2-propanediol to propanone and the other is conversion to propanal as shown in Figures 4.6 and 4.7, respectively. The first reaction path and ONIOM(B3LYP/6-31+G(d,p):AM1)-optimized structures of H-MOR catalyst as HZ and ZH are shown in Figure 4.6. It shows also the structures of interaction configurations with H-MOR in reaction pathway for 1,2-propanediol conversion to propanone. The second reaction path and the related ONIOM(B3LYP/6-31+G(d,p):AM1)-optimized structures are shown in Figure 4.7.

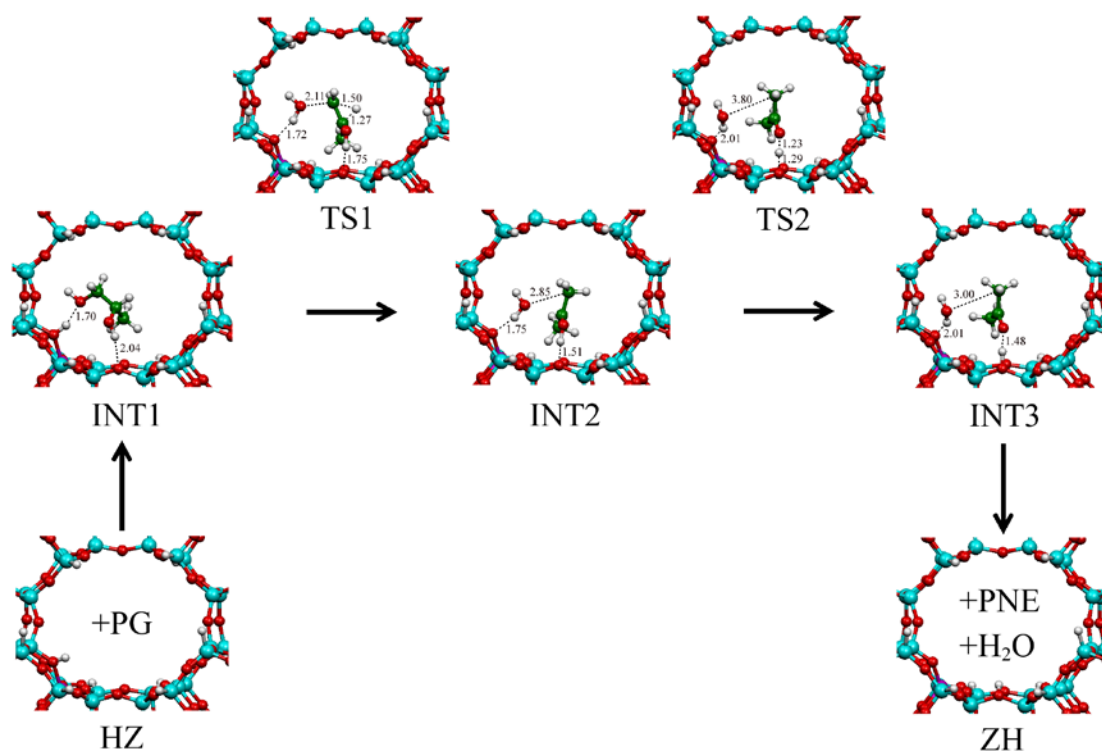


Figure 4.6. The ONIOM(B3LYP/6-31+G(d,p):AM1)-optimized structures of H-MOR catalyst and its interaction configurations in reaction pathway for 1,2-propanediol (PG) conversion to propanone (PNE). Bond distances are in Å.

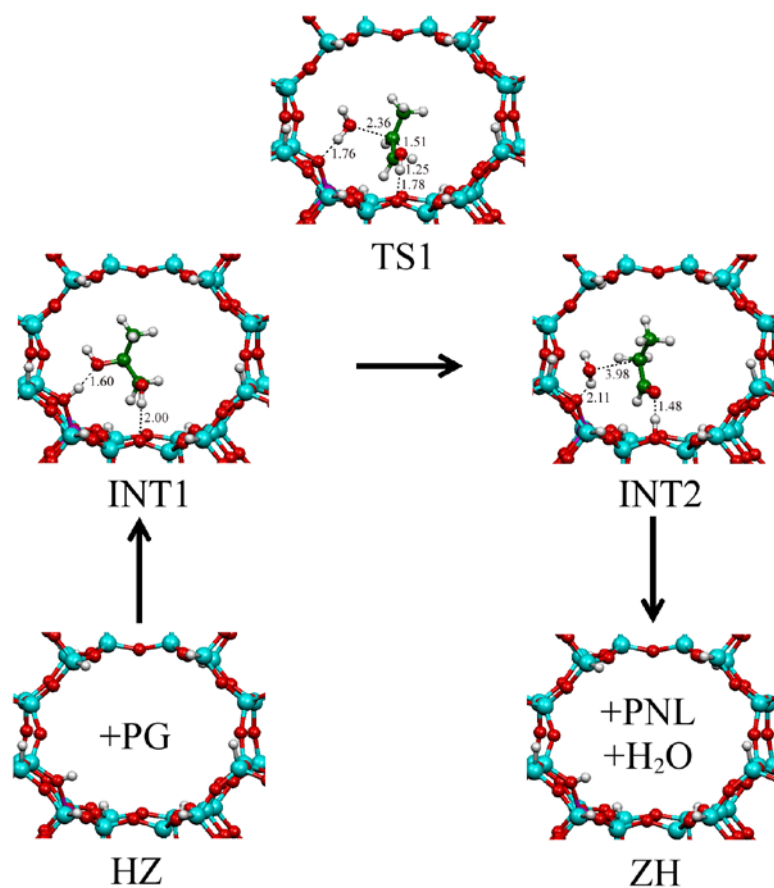


Figure 4.7. The ONIOM(B3LYP/6-31+G(d,p):AM1)-optimized structures of H-MOR catalyst and its interaction configurations in reaction pathway for 1,2-propanediol (PG) conversion to propanal (PNL). Bond distances are in Å.

Potential energy profiles for 1,2-propanediol conversion to propanone and to propanal over the H-MOR catalyst are shown in Figures 4.8(a) and (b), respectively. The conversion of 1,2-propanediol conversion to propanone is also composed of four reaction steps. The first step, 1,2-propanediol adsorbs onto the H-MOR by pointing hydroxyl oxygen of hydroxyl group at the 1-position carbon atom toward the acid proton of H-MOR and pointing hydroxyl hydrogen atom of the other hydroxyl group toward oxygen atom of the H-MOR, shown as INT1 in Figure 4.6. The second step, the intermediate reactant INT1 affords the intermediate INT2 via transition state TS1. One water molecule was formed and bound to H-MOR oxygen atom. This step is therefore a dehydration step. The hydrogen-bond length, in INT1 (2.04 Å) is longer than that in INT2 (1.51 Å) by 0.53 Å. This means that [H...O] hydrogen-bond in INT2 is stronger than that in INT1 because of the [H...O] in INT2 is a single hydrogen bonding with positive charge. The third step, the intermediate reactant INT2 affords the intermediate INT3 via transition state TS2. This step is the proton transfer process in order to retain the H-MOR as ZH. The last step is the desorption process of water and propanone as final product.

The conversion of 1,2-propanediol conversion to propanal comprises three reaction steps. The first step, 1,2-propanediol adsorbs onto the H-MOR by pointing hydroxyl oxygen of hydroxyl group at the 2-position carbon atom toward the acid proton of H-MOR and pointing hydroxyl hydrogen atom of the other hydroxyl group toward oxygen atom of the H-MOR, shown as INT1 in Figure 4.7. The second step, the intermediate reactant INT1 affords the intermediate INT2 via transition state TS1 and one water molecule was formed and bound to H-MOR oxygen atom. The hydrogen-bond length, in INT1 (2.00 Å) is longer than that in INT2 (1.48 Å) by 0.52 Å. The last step is the desorption process to afford propanal product.

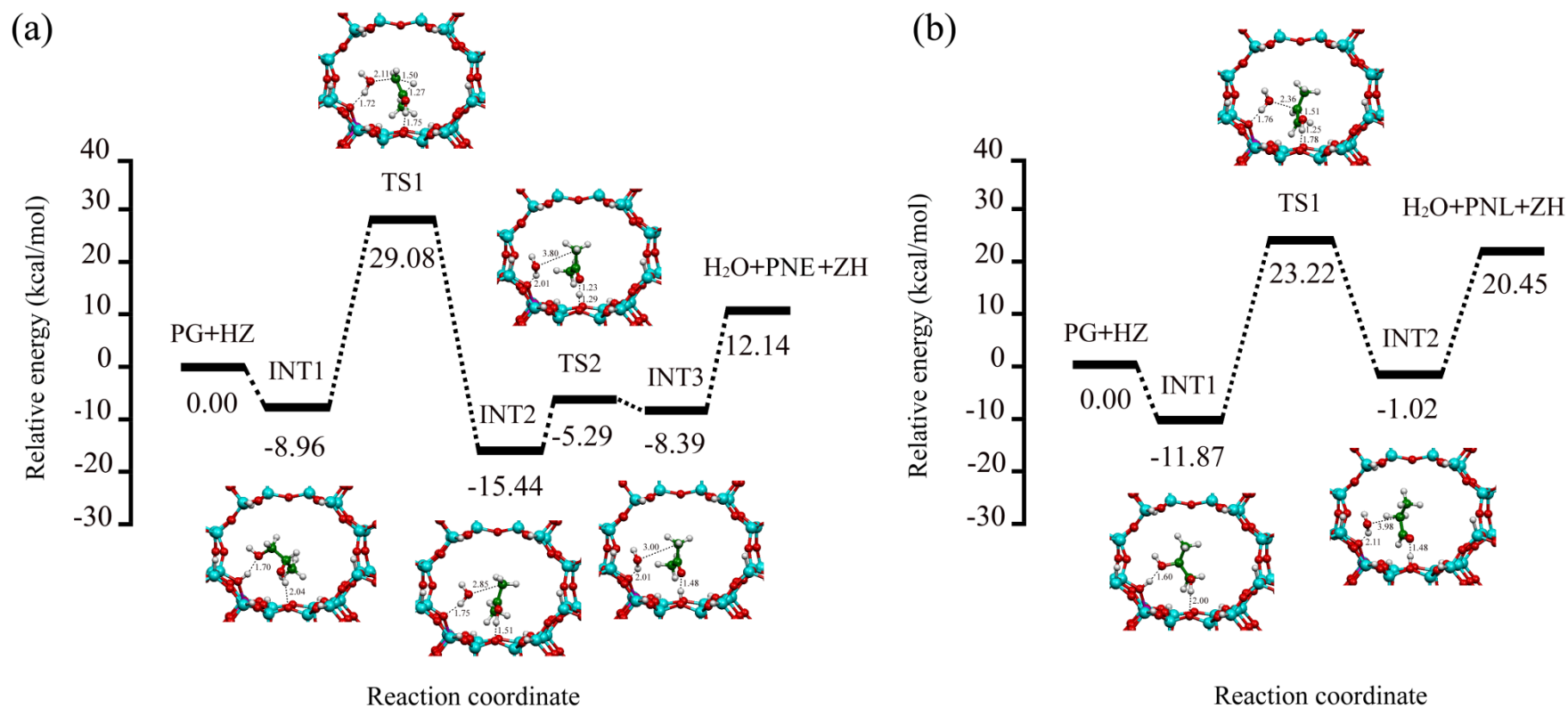


Figure 4.8. Potential energy profiles for (a) 1,2-propanediol (PG) conversion to propanone (PNE) and (b) 1,2-propanediol (PG) conversion to (PNL) over the H-MOR catalyst. Bond distances are in Å.

Table 4.2 shows that the rate determining steps for the propanone and propanal pathway are 5.78×10^{-16} and $4.18 \times 10^{-12} \text{ s}^{-1}$, respectively. The overall equilibrium constants for the propanone and propanal pathways are 1.70×10^{-4} and 4.10×10^{-8} , respectively. The overall reaction enthalpies of both pathways are exothermic process.

Table 4.2 Reaction energies, thermodynamic properties, rate constants and equilibrium constants for conversion reactions of 1,2-propanediol (PG) to propanone (PNE) and propanal (PNL) over the H-MOR catalyst.

| Catalysts/Reactions ^a | $\Delta^\ddagger E$ ^{a,b} | $\Delta^\ddagger G$ ^{a,b} | k_{298} ^c | ΔE ^a | ΔH_{298} ^a | ΔG_{298} ^a | K_{298} |
|--------------------------------------|------------------------------------|------------------------------------|------------------------|-------------------------|-------------------------------|-------------------------------|-----------------------|
| <i>Pathway for Propanone:</i> | | | | | | | |
| PG + HZ → INT1 | – | – | – | –8.96 | –8.85 | 3.28 | 3.93×10^{-3} |
| INT1 → TS1 → INT2 | 38.05 | 38.50 | 5.78×10^{-16} | –6.47 | –5.95 | –6.08 | 2.88×10^4 |
| INT2 → TS2 → INT3 | 10.15 | 8.98 | 3.22×10^6 | 7.04 | 10.35 | 8.98 | 2.60×10^{-7} |
| INT3 → PNE + H ₂ O + ZH | – | – | – | 20.54 | 21.26 | –1.04 | 5.77×10^0 |
| <i>Pathway for Propanal:</i> | | | | | | | |
| PG + HZ → INT1 | – | – | – | –11.87 | –11.90 | 1.32 | 1.07×10^{-1} |
| INT1 → TS1 → INT2 | 35.09 | 33.20 | 4.18×10^{-12} | 10.85 | 11.72 | 9.04 | 2.35×10^{-7} |
| INT2 → PNL + H ₂ O + ZH | – | – | – | 21.47 | 22.16 | –0.30 | 1.66×10^0 |

^a Computed at ONIOM(B3LYP/6–31+G(d,p):AM1) level, in kcal mol^{–1}.

^b Activation energy.

^c In s^{–1}.

4.4 Conversion of 1,2-propanediol over the H-TON

The reaction mechanism of 1,2-propanediol over the H-TON was also found to consist of two reaction paths. One is the conversion of 1,2-propanediol to propanone and the other is conversion to propanal as shown in Figure 4.9 and 4.10, respectively. The first reaction path and ONIOM(B3LYP/6-31+G(d,p):AM1)-optimized structures of H-TON catalyst as HZ and ZH are shown in Figure 4.9. It shows also the structures of interaction configurations with H-TON in reaction pathway for 1,2-propanediol conversion to propanone. The second reaction path and the related ONIOM(B3LYP/6-31+G(d,p):AM1)-optimized structures are shown in Figure 4.10.

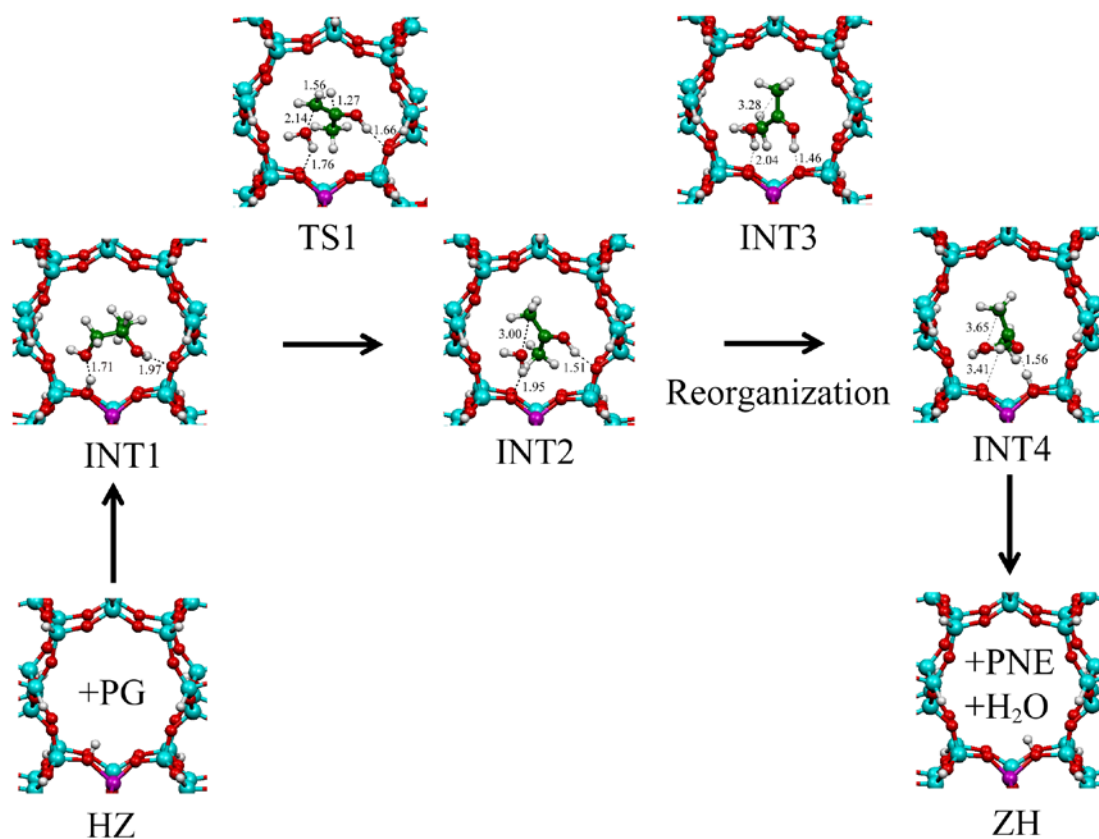


Figure 4.9. The ONIOM(B3LYP/6-31+G(d,p):AM1)-optimized structures of H-TON catalyst and its interaction configurations in reaction pathway for 1,2-propanediol (PG) conversion to propanone (PNE). Bond distances are in Å.

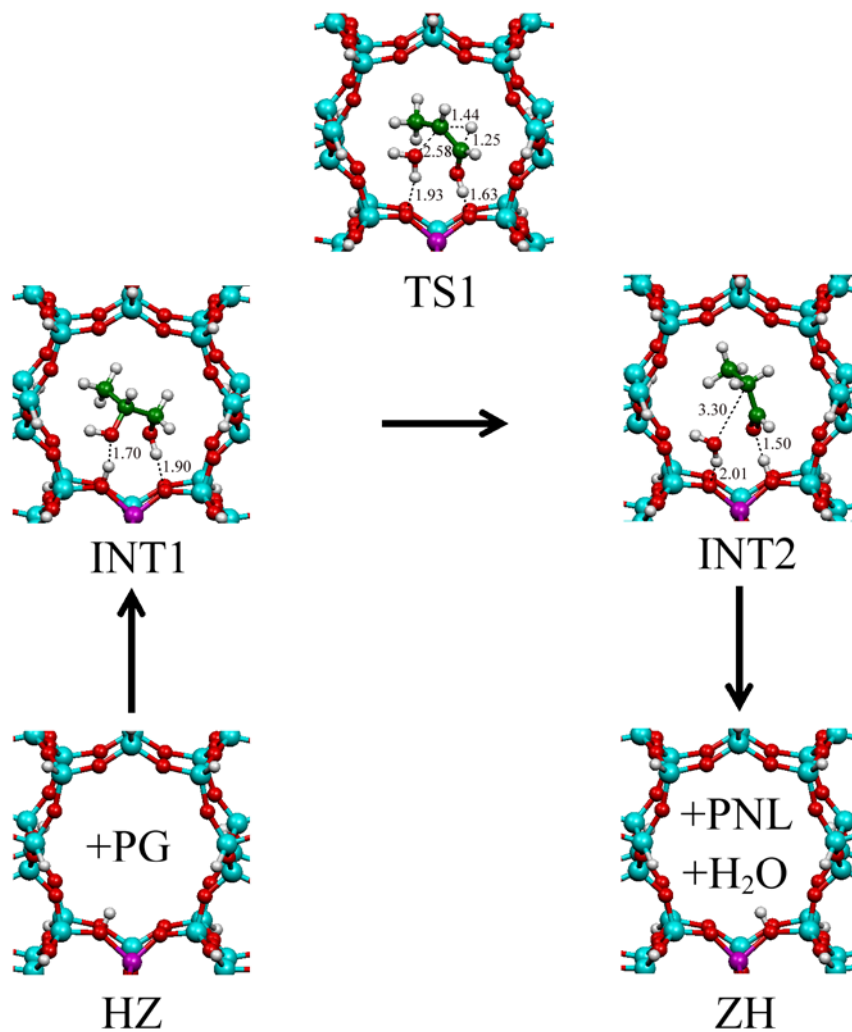


Figure 4.10. The ONIOM(B3LYP/6-31+G(d,p):AM1)-optimized structures of H-TON catalyst and its interaction configurations in reaction pathway for 1,2-propanediol (PG) conversion to propanal (PNL). Bond distances are in Å.

Potential energy profiles for 1,2-propanediol conversion to propanone and to propanal over the H-TON catalyst are shown in Figure 4.10(a) and (b), respectively. The conversion of 1,2-propanediol conversion to propanone is composed of five reaction steps. The first step, 1,2-propanediol adsorbs onto the H-TON by pointing hydroxyl oxygen of hydroxyl group at the 1-position carbon atom toward the acid proton of H-TON and pointing hydroxyl hydrogen atom of the other hydroxyl group toward oxygen atom of the H-TON, shown as INT1 in Figure 4.9. The second step, the intermediate reactant INT1 affords the intermediate INT2 via transition state TS1. One water molecule was formed and bound to H-TON oxygen atom. This step is therefore a dehydration step. The hydrogen-bond length, in INT1 (1.97 Å) is longer than that in INT2 (1.51 Å) by 0.46 Å. This means that [H···O] hydrogen-bond in INT2 is stronger than that in INT1 because of the [H···O] in INT2 is a single hydrogen bonding with positive charge. The third step, the intermediate reactant INT2 translates to the intermediate INT3. The fourth step, the hydroxyl proton of intermediate INT3 is transferred to zeolite affording the intermediate INT4. This step is the proton transfer process in order to retain the H-TON as ZH. The last step is the desorption process of water and propanone as final product.

The conversion of 1,2-propanediol conversion to propanal comprises three reaction steps. The first step, 1,2-propanediol adsorbs onto the H-TON by pointing hydroxyl oxygen of hydroxyl group at the 2-position carbon atom toward the acid proton of H-TON and pointing hydroxyl hydrogen atom of the other hydroxyl group toward oxygen atom of the H-TON, shown as INT1 in Figure 4.10. The second step (dehydration step), the intermediate reactant INT1 affords the intermediate INT2 via transition state TS1 and one water molecule was formed and bound to H-TON oxygen atom. The hydrogen-bond length, in INT1 (1.90 Å) is longer than that in INT2 (1.50 Å) by 0.40 Å. The last step is the desorption process to afford propanal product.

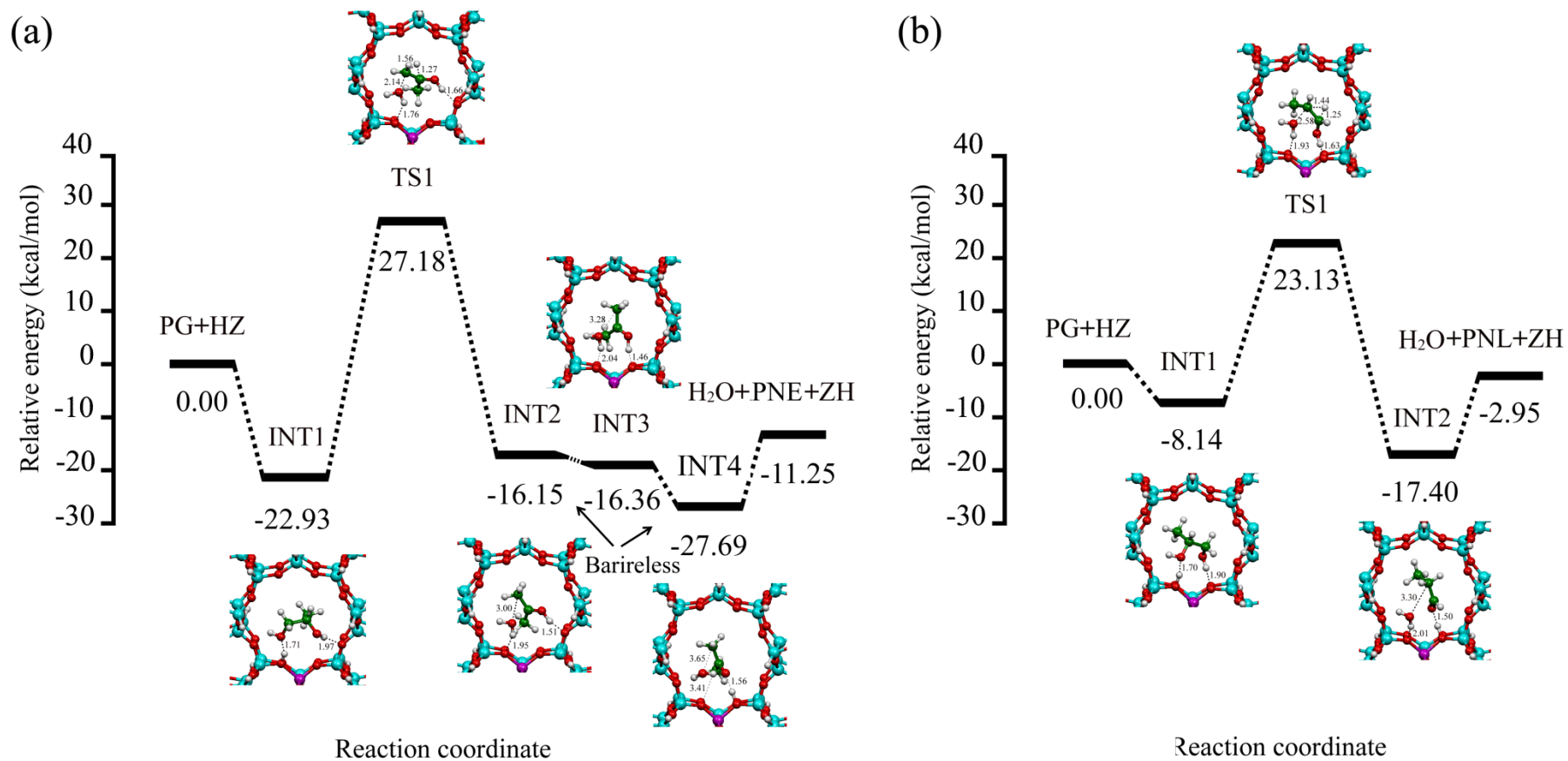


Figure 4.11. Potential energy profiles for (a) 1,2-propanediol (PG) conversion to propanone (PNE) and (b) 1,2-propanediol (PG) conversion to propanal (PNL) over the H-TON catalyst. Bond distances are in Å.

Table 4.3 shows that the rate determining steps for the propanone and propanal pathway are 2.04×10^{-24} and $5.20 \times 10^{-10} \text{ s}^{-1}$, respectively. The over all equilibrium constants for the propanone and propanal pathways are 3.00×10^{15} and 2.69×10^9 , respectively. The overall reaction enthalpies of both pathways are exothermic process.

Table 4.3 Reaction energies, thermodynamic properties, rate constants and equilibrium constants for conversion reactions of 1,2-propanediol (PG) to propanone (PNE) and propanal (PNL) over the H-TON catalyst.

| Catalysts/Reactions ^a | $\Delta^\ddagger E$ ^{a,b} | $\Delta^\ddagger G$ ^{a,b} | k_{298} ^c | ΔE ^a | ΔH_{298} ^a | ΔG_{298} ^a | K_{298} |
|--------------------------------------|------------------------------------|------------------------------------|--------------------------|-------------------------|-------------------------------|-------------------------------|-------------------------|
| <i>Pathway for Propanone:</i> | | | | | | | |
| PG + HZ → INT1 | – | – | – | -22.93 | -22.92 | -10.02 | 2.22 x 10 ⁷ |
| INT1 → TS1 → INT2 | 50.10 | 50.02 | 2.04 x 10 ⁻²⁴ | 6.77 | 7.70 | 6.01 | 3.94 x 10 ⁻⁵ |
| INT2 → INT3 | – | – | – | -0.20 | -1.01 | 1.32 | 1.08 x 10 ⁻¹ |
| INT3 → INT4 | – | – | – | -11.34 | -9.85 | -15.07 | 1.11 x 10 ¹¹ |
| INT4 → PNE + H ₂ O + ZH | – | – | – | 16.44 | 16.53 | -3.35 | 2.87 x 10 ² |
| <i>Pathway for Propanal:</i> | | | | | | | |
| PG + HZ → INT1 | – | – | – | -8.14 | -8.30 | 5.43 | 1.04 x 10 ⁻⁴ |
| INT1 → TS1 → INT2 | 31.27 | 30.34 | 5.20 x 10 ⁻¹⁰ | -9.26 | -8.05 | -11.12 | 1.42 x 10 ⁸ |
| INT2 → PNL + H ₂ O + ZH | – | – | – | 14.45 | 14.92 | -7.18 | 1.82 x 10 ⁵ |

^a Computed at ONIOM(B3LYP/6-31+G(d,p):AM1) level, in kcal mol⁻¹.

^b Activation energy.

^c In s⁻¹.

CHAPTER V

CONCLUSIONS

The reaction mechanisms of 1,2-propanediol over H-ZSM-5, H-MOR and H-TON catalysts were studied using ONIOM(B3LYP/6-31+G(d,p):AM1) method. The H-ZSM-5, H-MOR and H-TON structures were modeled as 52T, 68T and 68T clusters, respectively. It was found that the dehydration reactions of 1,2-propanediol over the H-ZSM-5, H-MOR and H-TON consist of two pathways. The first pathway is the conversion of 1,2-propanediol to propanone and the second one is the conversion to propanal.

The conversion reactions of 1,2-propanediol to propanone and propanal over the H-ZSM-5 catalyst, the rate determining step for the propanone pathway is the second step of which rate constant is $1.21 \times 10^{-12} \text{ s}^{-1}$ and for the propanal pathway is the second step of which rate constant is $4.09 \times 10^{-12} \text{ s}^{-1}$. The over all equilibrium constants for the propanone and propanal pathways are 1.71×10^{-2} and 8.53×10^{-8} , respectively. The overall reaction enthalpies of both pathways are exothermic process. For, the conversion reactions of 1,2-propanediol to propanone and propanal over the H-MOR catalyst, the rate determining step for the propanone and propanal pathways are 5.78×10^{-16} and $4.18 \times 10^{-12} \text{ s}^{-1}$, respectively. The over all equilibrium constants for the propanone and propanal pathways are 1.70×10^{-4} and 4.10×10^{-8} , respectively. The overall reaction enthalpies of both pathways are exothermic process. For, the conversion reactions of 1,2-propanediol to propanone and propanal over the H-TON catalyst, the rate determining step for the propanone and propanal pathways are $2.04 \times 10^{-24} \text{ s}^{-1}$ and $5.20 \times 10^{-10} \text{ s}^{-1}$, respectively. The over all equilibrium constants for the propanone and propanal pathways are 3.00×10^{15} and 2.69×10^9 , respectively. The overall reaction enthalpies of both pathways are exothermic process.

The rate constants for 1,2-propanediol conversion to propanal and 1,2-propanediol conversion to propanone over all studied zeolites are in decreasing order: H-TON > H-ZSM-5 > H-MOR and H-ZSM-5 > H-MOR > H-TON, respectively.

These results corresponds to the experiment [28] which the H-TON and H-ZSM-5 are the best catalysts for conversion of 1,2-propanediol to propanal and propanone, respectively.

REFERENCES

- [1] Imanaka, T., Okamoto, Y., and Teranishi, S. The isomerization of propylene oxide on metal phosphate catalysts. Bull. Chem. Soc. Japan. 45 (1972): 1353–1357.
- [2] Bron, M., et al. Silver as acrolein hydrogenation catalyst: Intricate effects of catalyst nature and reactant partial pressures (Review). Phys. Chem. Chem. Phys. 9 (2007): 3559–3569.
- [3] Zapirtan, V.I., Mojet, B.L., Van Ommen, J.G., Spitzer, J., and Lefferts, L. Gas phase hydroformylation of ethylene using organometallic Rh-complexes as heterogeneous catalysts. Catal. Lett. 101 (2005): 43–47.
- [4] Isidorov, V.A., Zenkevkh, I.G., and Ioffe, B.V. Volatile organic compounds in the atmosphere of forests. Atmos. Environ. 19 (1985): 1–8.
- [5] Goldstein, A.H., and Schade, G.W. Quantifying biogenic and anthropogenic contributions to acetone mixing ratios in a rural environment. Atmos. Environ. 34 (2000): 4997–5006.
- [6] Singh, H.B., et al. Acetone in the atmosphere distribution, sources and sinks. Jour. Geophys. Res. 99 (1984): 1805–1819.
- [7] Khandan, N., Kazemeini, M., and Aghaziarati, M. Determining an optimum catalyst for liquid-phase dehydration of methanol to dimethyl ether. Appl. Catal. A: Gen. 349 (2008): 6–12.
- [8] Chiang, H., and Bhan, A. Catalytic consequences of hydroxyl group location the rate and mechanism of parallel dehydration reactions of ethanol over acidic zeolites. J. Catal. 271 (2010): 251–261.
- [9] Ramesh, K., Jie, C., Han, Y.F., and Borgna, A. Synthesis, characterization, and catalytic activity of phosphorus modified H-ZSM-5 catalysts in selective ethanol dehydration. Ind. Eng. Chem. Res. 49 (2010): 4080–4090.
- [10] Bi, J., Guo, X., Liu, M., and Wang, X. High effective dehydration of bio-ethanol into ethylene over nanoscale HZSM-5 zeolite catalysts. Catal. Today. 149 (2010): 143–147.

- [11] Laak, A.N.C. et al. Alkaline treatment on commercially available aluminum rich mordenite. Appl. Catal. A: Gen. 382 (2010): 65–72.
- [12] Farneth, W.E., and Gorte, R.J. Methods for characterizing zeolite acidity. Chem. Rev. 93 (1995): 615–635.
- [13] Valyon, J., Onyestyák, G., and Rees, L.V.C. Study of the dynamics of NH₃ adsorption in ZSM–5 zeolites and the acidity of the sorption sites using the frequency–response technique. J. Phys. Chem. B. 102 (1998): 8994–9001.
- [14] Jinzhe, L. et al. Comparative study of MTO conversion over SAPO–34, H–ZSM–5 and H–ZSM–22: Correlating catalytic performance and reaction mechanism to zeolite topology. Catal. Today. 171 (2011): 221–228.
- [15] Wu, W., Guo, W., Xiao, W., and Luo, M. Dominant reaction pathway for methanol conversion to propene over high silicon H–ZSM–5. J. Chem. Eng. Sci. 66 (2011): 4722–4732.
- [16] Lónyi, F., and Valyon, J. A TPD and IR study of the surface species formed from ammonia on zeolite H–ZSM–5, H–mordenite and H–beta. Thermochim Acta. 373 (2001): 53–57.
- [17] Kapustin, G.I., and Brueva, T.R. A simple method for determination of heats of ammonia adsorption on catalysts from thermodesorption data. Thermochim Acta. 379 (2001): 71–75.
- [18] Brueva, T.R., Mishin, I.V., and Kapustin, G.I. Distribution of acid–site strengths in hydrogen zeolites and relationship between acidity and catalytic activity. Thermochim Acta. 389 (2001): 15–23.
- [19] Huo, H., Peng, L., Gan Z., and Grey C.P. Solid–state MAS NMR studies of Brønsted acid sites in zeolite H–mordenite. J. Am. Chem. Soc. 134 (2012): 9708–9720.
- [20] Onida, B., et al. IR evidence that secondary interactions may hamper H–bonding at protonic sites in zeolites. J. Phys. Chem. B. 106 (2002): 10518–10522.

- [21] Redondo, A., Hay, P.J. Quantum chemical studies of acid sites in zeolite ZSM-5. J. Phys. Chem. 97 (1993): 11754-11761.
- [22] Chatterjee, A., Iwasaki, T., Ebina T., and Miyamoto, A. Density functional study for estimating Brønsted acid site strength in isomorphously substituted ZSM-5. Micro. Meso. Mat. 21 (1998): 421-428.
- [23] Chatterjee, A. and Vetrivel, R. Computer simulation studies on the role of templating organic molecules in the synthesis of ZSM-5. J. Chem. Soc. 91 (1995): 4313-4319.
- [24] Yuan, S.P., Wang, J.G., Li, Y.W., and Jiao, H. Density functional investigations into the siting of Fe and the acidic properties of isomorphously substituted mordenite by B, Al, Ga and Fe. J. Mol. Struct. Theochem. 674 (2004): 267-274.
- [25] Geobaldo, F., et al. An FTIR Study of Zeolite Theta-1. J. Phys. Chem. B. 107 (2003): 1258-1262.
- [26] Derewinski, M., Sarv, P., and Mifsud, A. Thermal stability and siting of aluminum in isostructural ZSM-22 and Theta-1 zeolites. Catal. Today. 114 (2006): 197-204.
- [27] Jansen, A. and Ruangpornvisuti, V. An ONIOM investigation of reaction mechanism of propylene glycol dehydration over H-ZSM-5 and H-MOR catalysts. J. Mol. Catal. A: Chem. 363-364 (2012): 171-177.
- [28] Zhang, D., Barri, S.A.I., and Chadwick, D. Dehydration of 1,2-propanediol to propionaldehyde over zeolite catalysts. Appl. Catal. A: Gen. 400 (2011): 148-155.
- [29] Bucsi, I., Molnár, A., and Bartók, M. Transformation of 1,3-, 1,4- and 1,5-diols over perfluorinated resinsulfonic acids (Nation-H). Tetrahedron. 51 (1995): 3319-3326.
- [30] Levine, Ira N. Quantum chemistry, Third edition. New York: Allyn and Bacon, 1983.
- [31] Mueller, Michael. Fundamental of quantum chemistry: molecular spectroscopy and modern electronic structure computation. New York: Kluwer Academic, 2001.

- [32] Young, D.C. Computational chemistry: A practical guide for applying techniques to real world problems. New York: John Wiley and Sons 2001.
- [33] Wigner, E., and Hirschfelder, J.O. Some quantum–mechanical considerations in the theory of reactions involving and activation energy. J. Chem. Phys. 7 (1939): 616–628.
- [34] Yuan, S.P., Wang, J.G., Li, Y.W., and Jiao, H. Density functional investigations into the siting of Fe and the acidic properties of isomorphously substituted mordenite by B, Al, Ga and Fe. J. Mol. Struct. Theochem. 674 (2004): 267–274.
- [35] Ochterski, J.W. Thermochemistry in Gaussian. Gaussian Inc., 2000.
- [36] Maseras, F., and Morokuma, K. IMOMM: A new integrated *ab initio* + molecular mechanics geometry optimization scheme of equilibrium structures and transition states. J. Comp. Chem. 16 (1995): 1170–1179.
- [37] Humbel, S., Sieber, S., and Morokuma, K. The IMOMO method: Integration of different levels of molecular orbital approximations for geometry optimization of large systems: Test for n–butane conformation and S_N2 reaction: RCl+Cl⁻. J. Chem. Phys. 105 (1006): 1959–1967.
- [38] Becke, A.D. Density–functional thermochemistry. III. The role of exact exchange. J. Chem. Phys. 98 (1993): 5648–5652.
- [39] Lee, C., Yang, W., and Parr, R.G. Development of the Colle–Salvetti correlation–energy formula into a functional of the electron density. Phys. Rev. B. 37 (1998): 785–789.
- [40] McLean, A.D., and Chandler, G.S. Contracted Gaussian basis sets for molecular calculations. I. Second row atoms, Z=11–18. J. Chem. Phys. 72 (1980): 5639–5648.
- [41] Dewar, M. J. S., and Reynolds, C.H. An improved set of mndo parameters for sulfur. J. Comp. Chem. 7 (1986): 140–143.
- [42] Koningsveld, H.V., Bekkum, and H.V., Jansen, J.C. Acta Cryst. B. 43 (1987): 127–132.

- [43] Baerlocher, Ch., McCusker, L.B., and Olson, D.H. Atlas of Zeolite Structure Types, Second edition. Elsevier, Amsterdam, Boston, Heidelberg, London, New York, Oxford, Paris, San Diego, San Francisco, Singapore, Sydney, Tokyo. (2007).
- [44] Mallinson, P. R. Electron density dictionary. International tables for crystallography. (2005).
- [45] Peng, C., Ayala, P.Y., Schlegel, H.B., and Frisch, M.J. Using redundant internal coordinates to optimize equilibrium geometries and transition states. J. Comp. Chem. 17 (1996): 49–56.
- [46] Pu, S.–B., and Inui, T. Zeolites. 19 (1997): 452–454.

VITAE

Name: Miss ARUNWAN JANSEN

Date of Birth: November 10th, 1986

Place of Birth: Chachoengsao, Thailand

Address: 133 Nongyao, Phanomsarakham, Chachoengsao 24120, Thailand

Telephone: 084-5672637

E-mail address: arun-wan@hotmail.com

Educations:

2010–2012 M.Sc. (Petrochemistry and Polymer Science), Chulalongkorn University, Thailand

2005–2008 B.Sc. (Chemistry), Burapha University, Thailand

1999–2004 Phanomsarakham “Phanom Adul Vitthaya” high school, Chachoengsao, Thailand

1993–1998 Wathakwian (Saiuthit) primary school, Chachoengsao, Thailand

Scholaship:

2012 The 90th Anniversary of Chulalongkorn University Fund (Ratchadaphiseksomphot Endowment Fund) provided through the Graduate School, Chulalongkorn University

Publication:

Jansen, A., and Ruangpornvisuti, V. An ONIOM investigation of reaction mechanism of propylene glycol dehydration over H-ZSM-5 and H-MOR catalysts. J. Mol. Catal. A: Chem. 363–364 (2012): 171–177.